Via-Hole Technology for High Efficiency Millimeter Wave Antennas and Wafer Scale Integration

(Microwave and Millimeter Wave Tapered Slot Antennas on High ε_r and Low ε_r Micromachined Dielectric Substrates)

Final Progress Report

Prof. Gabriel M. Rebeiz (PI)
Thomas J. Ellis (GSRA)
Jeremy B. Muldavin (GSRA)

July 13, 1998

U.S. Army Research Office

Contract: DAAL04-94-G-0137
7/1/94 – 12/31/97

The Radiation Laboratory
EECS Department
The University of Michigan
Ann Arbor, Michigan
48109-2122

31943-1-F = RL-2448

REPORT DOCUMENTATION PAGE

Form Approved
OMB NO. 0704-0188

1. AGENCY USE ONLY (Leave blank)	2. REPORT DATE	3. REPORT TYPE AND DATES COVERED
	7/13/98	Final Progress Report, 7/94 - 12/31/97

4. TITLE AND SUBTITLE
Via-Hole Technology for High Efficiency Millimeter Wave Antennas and Wafer Scale Integration

5. FUNDING NUMBERS
DAAH04-94-G-0137
P-3277-EL-AAS

6. AUTHOR(S)
Professor Gabriel M. Rebeiz, Thomas J. Ellis, Jeremy B. Muldavin

7. PERFORMING ORGANIZATION NAME(S) AND ADDRESS(ES)
University of Michigan
EECS, Radiation Lab.
130l Beal Avenue
Ann Arbor, Michigan 48109-2122

8. PERFORMING ORGANIZATION REPORT NUMBER
031943-F-1

9. SPONSORING / MONITORING AGENCY NAMES(S) AND ADDRESS(ES)
Department of the Army
Army Research Office
P.O. Box 12211
Research Triangle Park, NC 27709-2211

10. SPONSORING / MONITORING AGENCY REPORT NUMBER

11. SUPLEMENTARY NOTES
The views, opinions and/or findings contained in this report are those of the author(s) and should not be construed as an official Department of the Army position, policy or decision, unless so designated by other documentation.

12a. DISTRIBUTION / AVAILABILITY STATEMENT
Approved for public release; distribution unlimited.

12b. DISTRIBUTION CODE

13. ABSTRACT (Maximum 200 words)

Via-hole technology has been investigated on low-epsilon_r and high-epsilon_r substrates as a means of improving the patterns and efficiency of tapered-slot antennas. The via-holes are achieved either using a numerically controlled milling machine in Duroid, or using micromachining techniques in silicon wafers. Experiments were conducted at 10 Ghz, 30 GHz and 94 Ghz on low and high-epsilon_r substrates. We have proven that for low-epsilon_r substrates, the effect is purely a quasi-static reduction of the dielectric constant, while for high-epsilon_r substrates, the effect is both quasi-static and a significant disruption of substrate modes, thereby resulting in much improved patterns and efficiencies. A micromachined constant-width tapered slot antenna was fabricated at 94 GHz and resulted in excellent patterns suitable for mm-wave imaging arrays.

14. SUBJECT TERMS

15. NUMBER IF PAGES

16. PRICE CODE

17. SECURITY CLASSIFICATION OR REPORT	18. SECURITY CLASSIFICATION OF THIS PAGE	19. SECURITY CLASSIFICATION OF ABSTRACT	20. LIMITATION OF ABSTRACT
UNCLASSIFIED	UNCLASSIFIED	UNCLASSIFIED	UL

1. Foreword

None.

2. Table of Contents

None

3. List of Appendixes

Appendix A: Copies of papers published with the support of this contract.

"MM-Wave Tapered Slot Antennas on Micromachined Photonic Bandgap Dielectrics", T.J.Ellis, G.M.Rebeiz, 1996 *IEEE* MTT-S Int Microwave Symp, Conference Proceeding, pp. 1157-1161

"Improvements in Tapered Slot Antennas on Thick Dielectric Substrates Using Micromachining Techniques"T.J.Ellis, G.M.Rebeiz, 1996 *IEEE* AP/URSI Antenna and Propagation Symp, Conference Proceedings, pp. 992-996

"Integration of Tapered Slot Antennas on MMIC Substrates Through Dielectric Micromachining", T.J.Ellis, G.M.Rebeiz, 1996 Air Force Research Lab Antenna Application Symp, Conference Proceedings

"Tapered Slot Antennas on Thick Dielectric Substrates Using Micromachining Techniques", J.B.Muldavin, G.M.Rebeiz, 1997 *IEEE* AP/URSI Antenna and Propagation Symp, Conference Proceedings, pp. 1110-1113

"MM-Wave Tapered Slot Antennas on Synthesized Low Permittivity Substrates" J.B.Muldavin, G.M.Rebeiz, Submitted June, 1998 to the *IEEE* Transactions on Antennas and Propagation

4A. Statement of the Problem Studied

The goal of this project was to develop high efficiency microwave and millimeter wave antennas using the standard via-hole technologies available in today's IC fabrication processes. The effects of "bulk" (i.e. large area or entire wafer) micromachining dielectric substrates was investigated to determine the effects such a process would have on the radiation properties of printed antennas.

It was originally anticipated that the micromachining would have the singular effect of lowering the "effective" or quasi-static dielectric constant of the substrate, making it possible to integrate the antennas onto thick, high dielectric constant substrates.

4B. Summary of the Most Important Results

The introduction of via-holes (non-metalized) into the substrate had a significant effect on the radiation properties of the tapered slot antennas (TSA) on thick dielectric

substrates. A significant improvement in the radiated far field patterns was noted, with the measured directivity increasing on the order of 85 to 165 %, depending on the substrate used. The radiation efficiency also showed dramatic improvement, with increases in the 50% to 80% range measured. It has been concluded that the improvements can be attributed to two separate mechanisms resulting from the micromachining.

1) Lower Dielectric Constant (applicable to both high and low permittivity substrates): The introduction of large numbers of relatively small holes into the substrates removes a given volume of the dielectric material. Assuming the holes are smaller than a wavelength ($d \cong \lambda_o/5$), a quasi-static dielectric mixing model can be assumed valid and used to predict an "effective" dielectric constant based on the volume of material removed. Not only has the effective dielectric constant been reduced, but since much of the material has been replaced by air, the loss tangent of the material has also been reduced. For the tapered slot antenna, the micromachined substrate appears to be electrically thinner and not as lossy as the original substrate. This effect was seen in both the low ε_r and high ε_r materials investigated.

2) Substrate Mode Reduction (applicable to only high permittivity substrates): To ensure a uniform dielectric constant for the micromachined substrate, the holes were arranged in uniform, periodic arrays. The holes, being discontinuities in the dielectric, alter the propagation function (i.e. Green's Function) of the substrate. An exact solution to the problem of periodic holes in a finite dielectric material is not available, and it is the focus of current research efforts. The effects of the micromachining, however, appear to be a significant disruption to the formation and propagation of substrate modes. This conclusion was drawn for a number of reasons.

First, the radiation patterns of the TSA suffer from interference from the surface waves that form if thick, high ε_r substrates are used. The overall radiation efficiency also suffers as energy is coupled away from the desired signal and into substrate modes. The radiation patterns and efficiency were increased significantly more on the high ε_r substrates, as compared to the low ε_r materials. Since surface wave excitation is greater on the high ε_r materials, any reduction in surface wave excitation would be greater on the high ε_r substrates.

Second, to ensure that the improvements recorded for the TSA on the high ε_r substrates was not due only to the quasi-static reduction in ε_r, a TSA was fabricated on a quartz substrate. Quartz was chosen because it has approximately the same dielectric constant that the micromachined high ε_r substrate had been machined to. The resulting measurements showed that the micromachined TSA had better radiation efficiency and far field patterns than the same TSA on quartz, which led to the conclusion that the disruption to the surface waves was the cause of the additional improvements.

Third, the micromachined substrates have a geometry that is quite similar to a class of materials that exhibit a phenomenon known as "Photonic Bandgap". While the micromachined substrate developed has many differences to classic "PBG" substrates, it does seem to exhibit similar properties. The most significant similarity being that the hole geometry (size and arrangement) is important for optimizing the reduction of surface waves. It was found experimentally that a rectangular lattice arrangement rotated 45° to the end-fire direction of the TSA resulted in the most improvement in the measured efficiency and patterns.

4C. List of All Publications and Technical Reports

1 - "MM-Wave Tapered Slot Antennas on Micromachined Photonic Bandgap Dielectrics", T.J.Ellis, G.M.Rebeiz, 1996 *IEEE* MTT-S Int Microwave Symp, Conference Proceeding, pp. 1157-1161

2 - "Improvements in Tapered Slot Antennas on Thick Dielectric Substrates Using Micromachining Techniques"T.J.Ellis, G.M.Rebeiz, 1996 *IEEE* AP/URSI Antenna and Propagation Symp, Conference Proceedings, pp. 992-996

3 - "Integration of Tapered Slot Antennas on MMIC Substrates Through Dielectric Micromachining", T.J.Ellis, G.M.Rebeiz, 1996 Air Force Research Lab Antenna Application Symp, Conference Proceedings

4 - "Tapered Slot Antennas on Thick Dielectric Substrates Using Micromachining Techniques", J.B.Muldavin, G.M.Rebeiz, 1997 *IEEE* AP/URSI Antenna and Propagation Symp, Conference Proceedings, pp. 1110-1113

5 - Final SBIR Report to Millimetrix, Inc. September 1997

6 - "MM-Wave Tapered Slot Antennas on Synthesized Low Permittivity Substrates" J.B.Muldavin, G.M.Rebeiz, Submitted June, 1998 to the *IEEE* Transactions on Antennas and Propagation

4d. List of all Participating Scientific Personnel

Professor Gabriel M. Rebeiz

Thomas J. Ellis Ph.D. Candidate; Expected Graduation Date: December 1998

Jeremy B. Muldavin M.S. Electrical Engineering, May 1998; Ph.D. Candidate

5. Report of Invention

"Improvement of Tapered Slot Antenna Patterns and Radiation Efficiencies Using Synthesized Dielectric Substrates"*

- no patent application has been filed

6. Bibliography

None.

7. Appendixes

Attached

IEEE Int. Microwave Theory and Techniques Symposium, June 1996, pp. 1157-1161

MM-Wave Tapered Slot Antennas on Micromachined Photonic Bandgap Dielectrics

Thomas J. Ellis and Gabriel M. Rebeiz

Radiation Laboratory
Electrical Engineering and Computer Science Department
University of Michigan, Ann Arbor, Michigan 48109
tellis@engin.umich.edu , rebeiz@engin.umich.edu

Abstract - **Dramatic improvements in the radiation properties of tapered slot antennas (TSA) integrated on high dielectric constant substrates have been achieved through micromachining techniques. A periodic hole structure was micromachined into the substrate converting it into a photonic bandgap material. The measured directivity of a $4\lambda_0$ TSA on a 50 mil (1.27mm) thick Duroid substrate (ε_r = 10.5) was increased by 240% using micromachined holes with a hexagonal geometry. A similar improvement was observed when the process was performed at 30 GHz on a 14 mil (350 μm) silicon wafer. We believe the technology can be scaled to 60 GHz and 94 GHz for communication systems, low-cost millimeter wave imaging arrays, and power combining systems.**

I. INTRODUCTION

The tapered slot antenna, sometimes referred to as the "Vivaldi" antenna, was first introduced by Gibson in 1979 [1]. Yngvesson et al. have published many papers on this antenna and have introduced several variations, including the "Constant Width Slot Antenna" and the "Broken Linear Tapered Slot Antenna" [2,3]. The TSA has also been theoretically analyzed by Janaswamy and Schaubert with excellent results for electrically thin dielectric substrates [4]. One of the main problems with the TSA is its sensitivity to the thickness of the supporting substrate. The "effective" thickness of the substrate has been defined as:

$$t_{eff} = t(\sqrt{\varepsilon_r} - 1) \qquad (1)$$

and represents the electrical thickness of the dielectric material supporting the antenna. It has been previously reported that the range of "effective" thickness for good operation of a TSA is approximately:

$$0.005 \le t_{eff}/\lambda_0 \le 0.03$$

This results in a very thin supporting structure for antennas at 30 GHz and above on high dielectric constant substrates such as Silicon or Gallium Arsenide. For a silicon carrier the maximum thickness allowed at 30 GHz is approximately 5 mils (120 μm). This makes the integration of a TSA somewhat impractical for commercial applications at millimeter-wave frequencies. One solution to this problem is to construct the antenna on a thin silicon nitride dielectric membrane. The membrane is only 1.5 μm thick and is compatible with silicon IC fabrication techniques. This technique has been successfully demonstrated at very high frequencies (348 GHz and 802 GHz) [5,6]. At lower frequencies, however, the membranes cannot be reliably fabricated to support the large surface areas required for the antennas.

In 1993, Brown et al. introduced the concept of photonic bandgap materials for slot and dipole antennas on dielectric substrates [7,8]. The idea is to etch a series of holes in a *stack* of Stycast wafers to synthesize a face-centered-cubic lattice structure within the dielectric. The photonic structure underneath the antenna resulted in large stop-bands for normally propagating waves, resulting in a large percentage of the power fed to the dipole to be radiated out into the space above the dielectric, greatly increasing the directivity of the antenna. We have expanded on this idea and developed Tapered Slot Antennas at 10 and 30 GHz on

dielectrics micromachined to disrupt substrate mode formation (Fig. 1). The results, presented in this paper, are the first known to the authors and show that the TSA can be successfully designed and operated on the thick dielectric substrates needed for commercially viable applications.

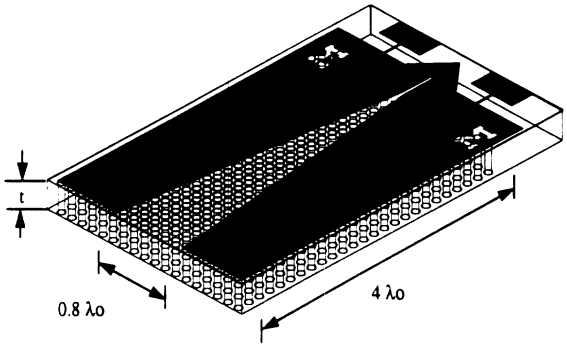

Fig. 1. Micromachined Tapered Slot Antenna

II. DESIGN

In this work we developed and tested four linearly tapered slot antennas with a center frequency of 10 GHz on Duroid, and one scaled version at 30 GHz on a high resistivity silicon substrate. All antennas are 4 λ_o long with a flare angle of 12°, resulting in an aperture width of 0.8 λ_o (Fig. 1). One antenna is made on a thin, low dielectric constant Duroid substrate (ε_r = 2.2) and is used as a reference antenna for performance comparison. Another antenna was fabricated on thick (50 mil), high dielectric constant Duroid (ε_r = 10.5). The last two were made on the same thick Duroid substrate but were machined with holes to suppress the substrate modes that are normally excited. Two different patterns of holes were machined, one with a rectangular geometry and the other with a hexagonal geometry (Fig. 2).

The calculated "effective" dielectric constant of the micromachined structures is

$$\varepsilon_{eff} = \varepsilon_r \left(1 - \frac{\pi D^2}{4 W^2} \right) \qquad (2)$$

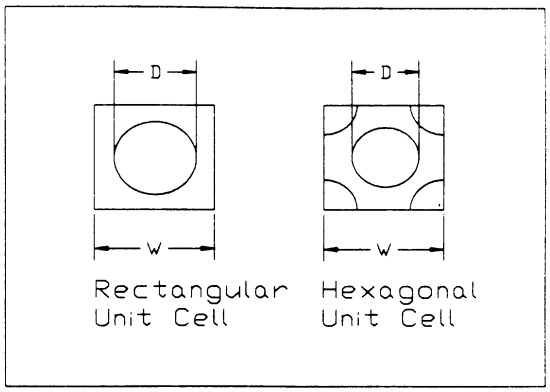

Fig. 2: Cell structure of the machined hole patterns.

for the rectangular geometry and

$$\varepsilon_{eff} = \varepsilon_r \left(1 - \frac{\pi D^2}{2 W^2} \right) \qquad (3)$$

for the hexagonal one. These values are based on quasi-static, volumetric principles. The above analysis was verified by the design and construction of transmission-line resonator elements on the machined substrates. The measured results agree quite well with the predicted values and confirm that the above "effective" dielectric constant is accurate. However, as will be shown in section III, the TSAs on micromachined dielectrics result in very good patterns even for large ε_{eff} and large t_{eff}/λ_0.

The antennas at 10 GHz are fabricated on 5" x 5" Duroid circuit boards (12.7cm x 12.7 cm). It is expected that energy coupled into substrate modes would eventually be radiated from the edges and the backside of the Duroid carrier. This stray energy will effect the directivity and patterns of the antenna. The Duroid material was machined using a CNC milling machine. The antennas were all fed with an 0.085" (2.16mm) coax line with the center conductor soldered across the slotline gap. The slotline feed is shorted $\lambda/4$ away (at 10 GHz) from the probe for best transition performance. The 30 GHz silicon TSA was tested by mounting a zero-bias schottky detector diode across the slot feed $\lambda/4$ away from an RF shorting capacitance All design parameters are listed in Table 1.

	Reference	Thick	Hexagonal	Rectangular
ε_r	2.2	10.5	10.5	10.5
t (mils)	30	50	50	50
ε_{eff}	2.2	10.5	9.6	8.4
t_{eff} / λ_o	0.012	0.095	0.081	0.089
W(mils)	---	---	125	200
D(mils)	---	---	125	200

Table 1: Design Parameters for 10 GHz TSA

III. 10 GHz MEASUREMENTS

The radiation patterns at 10 GHz for the antennas are shown in Fig.3-5 and the measured antenna properties are shown in Table 2. The patterns and directivity measured for the reference antenna (ε_r = 2.2 , t = 30 mils) agreed well with previously published results [1,2]. The antenna on the standard high dielectric constant material performed as poorly as expected with a directivity of 4.4 (compared to 13.7 for the reference antenna).

The directivity is calculated using:

$$D = \frac{4\pi U \max}{\iint (P_{co-pol} + P_{x-pol}) d\Omega} \qquad (4)$$

and the main beam efficiency is calculated using:

$$\eta_{main} = \frac{\iint P_{main-beam(-10dB)}}{\iint P_{total}} \qquad (5)$$

As seen in Figs 3-5, the antenna patterns on the micromachined substrates clearly show a dramatic improvements over the same antenna when supported by a standard high dielectric substrate.

There is a 240% increase in the directivity of the antenna when the supporting dielectric has been properly machined to suppress substrate modes (also note that the rectangular hole pattern showed an 81% increase in directivity, indicating that the geometry of the machining is important for optimum performance). This would make the TSA on high dielectric substrates suitable for medium size imaging arrays.

IV. 30 GHz MEASUREMENTS

A 30 GHz TSA was fabricated on 14 mil (350 μm) silicon substrate. The antenna was patterned and plated with gold to a thickness of 2 μm. The holes were etched using an HF Nitric solution and a silicon nitride masking layer. The process resulted in an anisotropic etch with nearly vertical sidewalls. This TSA has a rectangular geometry, with a hole diameter of 45 mils (1.14 mm) and spacing of 70mils (1.78 mm). The resulting effective dielectric constant is approximately 8. The measured pattern (Fig.6) shows again that substantial improvement can be achieved through the use of micromachined dielectric substrates (note that the improvement would have been greater had a hexagonal pattern been used for the holes). These improvements appears to be due not to the lower "effective" dielectric constant of the micromachined material but to the disruption of the dominate substrate modes imposed by the structure. Also, although the silicon wafer had been machined with holes it remained mechanically stable, was lighter, and should endure the types of environments required for commercial applications.

	Reference - ε_r=2.2	Thick - no holes - ε_r=10.5	Hexagonal holes - ε_r=10.5	Rectangular holes - ε_r=10.5
Directivity	13.7	4.4	14.9	8.0
Beamwidth (-10 dB)	E = 30° H = 45° D = 45°	E = 45° H = 90° D = 70°	E = 40° H = 45° D = 45°	E = 50° H = 65° D = 65°
X-Pol (45° Plane)	-7 dB	-7 dB	-13 dB	-10 dB
Main Beam η	50 %	57 %	57 %	60 %
F# lens	0.6	0.2	0.5	0.3

Table 2: Measurement Results of the 10 GHz TSA.

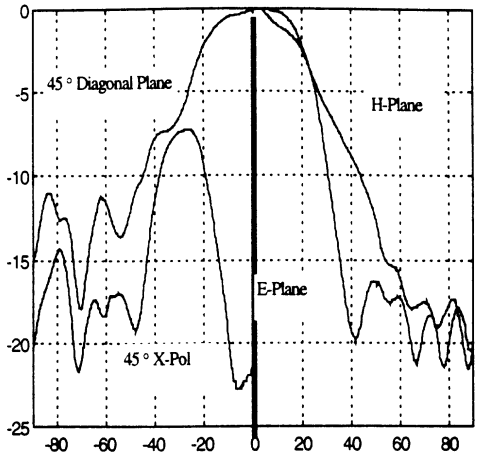

Fig. 3: Reference antenna patterns (ε_r=2.2) at 10 GHz.

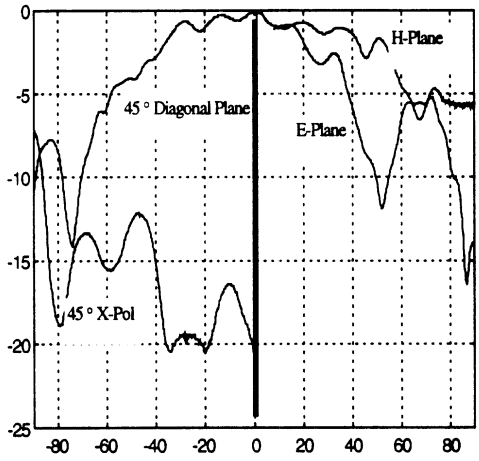

Fig. 4: Thick Duroid antenna patterns (ε_r=10.5) at 10 GHz.

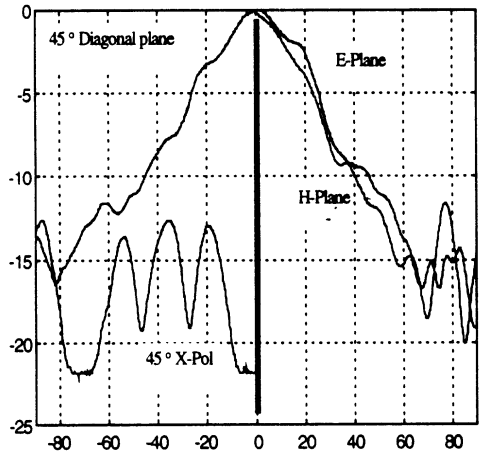

Fig. 5: Micromachined antenna patterns (ε_r=10.5) (Hexagonal hole geometry) at 10 GHz.

V. Acknowledgments

This work was supported by the Army Research Office under the contract #DAAL04-94-G-0137. We would also like to thank Rogers Corp. for their support in supplying the dielectric material needed for the 10 GHz antennas.

REFERENCES

[1] P.J.Gibson , "The Vilvaldi Aerial," *Proc. 9th European Microwave Conference*, 1979, pp.101-105.

[2] K.S.Yngvesson *et al.* , "Endfire Tapered Slot Antennas on Dielectric Substrates," *IEEE Trans. Antennas & Prop.*, vol.33, pp1392-1400, Dec 1985.

[3] K.S.Yngvesson *et al.*, "The Tapered Slot Antenna - A New Integrated Element for MM Wave Applications", *IEEE Trans. Microwave Theory & Tech.*, vol. 37, pp.365-374, Feb. 1989.

[4] R.Janaswamy and D.H.Schaubert, "Analysis of the Tapered Slot Antenna" *IEEE Trans. Antennas & Propagation*, vol.35, pp.1058-1065, Sept. 1987

[5] H.A.Ekstrom *et al*, "348 GHz Endfire Slotline Antennas on Thin Dielectric Membranes," *IEEE Microwave and Guided Letters"* vol.2, no.9, pp.357-358, Sept. 1992.

[6] P.Acharya *et al.* "Tapered Slot Antennas at 802 GHz," *IEEE Trans. Microwave Theory & Tech.*, vol. 41, pp.1715 - 1719, Oct. 1993.

[7] E.R.Brown and C.D.Parker, "Radiation Properties of a Planar Antenna on a Photonic-Crystal Substrate," *Journal of the Optical Society of America*, 1993.

[8] E.R.Brown and O.B.McMahon, "High Zenith Directivity from a Dipole Antenna on a Photonic Crystal," submitted to *Applied Physics Letters.*

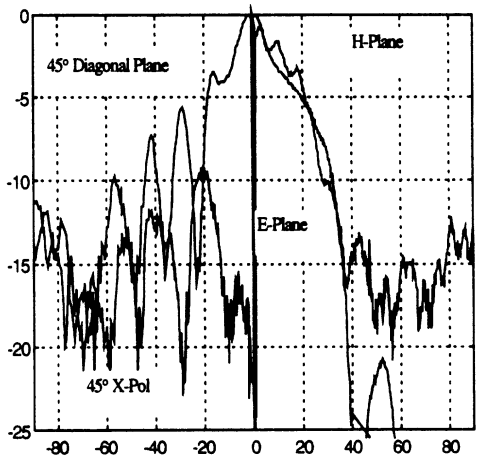

Fig. 6: TSA patterns on a thick (14 mil) micromachined silicon substrate with rectangular hole pattern at 30 GHz.

IEEE Int. Symposium on Antennas and Propagation, Baltimore, July 1996, pp. 992-996

Improvements in Tapered Slot Antennas on Thick Dielectric Substrates Using Micromachining Techniques

Thomas J. Ellis and Gabriel M. Rebeiz

Electrical Engineering and Computer Science Department
University of Michigan, Ann Arbor, Michigan 48109
tellis@engin.umich.edu , rebeiz@engin.umich.edu

Abstract - **The patterns of a Tapered Slot Antenna (TSA) on a thick (93 mils, 2.36 mm) low dielectric constant substrate (ε_r = 2.2) have been improved through micromachining techniques. A periodic hole structure was machined into the substrate to disrupt the formation of the dominate substrate modes. The measured directivity and main-beam efficiency of a $4\lambda_0$ long TSA was increased as a result of the micromachining. We believe that this technique will allow the TSA to operate on a much thicker dielectric substrate needed for inexpensive and commercially viable operations - particularly imaging and power combining arrays at 60 and 94 GHz.**

I. INTRODUCTION

The Tapered Slot Antenna on a thick, low dielectric constant substrate (ε_r=2.2) has been widely utilized in millimeter-wave imaging arrays at 94 GHz [1, 2]. One of the main drawbacks, however, is that the performance of the antenna is sensitive to the thickness of the supporting substrate. An "effective thickness" has been given to be

$$t_{eff} = t\left(\sqrt{\varepsilon_r} - 1\right)$$

and represents the electrical thickness of the substrate. One range for the "effective thickness" [3], normalized to the free-space wavelength, needed for good operation has been accepted to be approximately

$$0.005 \le t_{eff} / \lambda_0 \le 0.03$$

This results in the supporting dielectric being impractically thin at very high frequencies. A typical design at 94 GHz is a "Constant Width Slot Antenna" (CWSA) on an 80μm (3.15 mil) thick Duroid substrate (ε_r= 2.2). This yields a normalized effective thickness of 0.012 and is well within the range listed above. It would be advantageous to develop lower-cost and more mechanically stable designs using thicker 150μm (6 mil) and 250μm (10 mil) supporting substrates. This cannot currently be done using standard dielectrics because of substrate mode excitation within the dielectric substrate.

In 1993, Brown *et al.* introduced the concept of photonic bandgap materials for printed dipole antennas on dielectric substrates [4,5]. The photonic structure

resulted in large stop-bands in the material supporting the antennas which prohibited radiation from entering the substrate. We expanded on this idea and developed a TSA on a thick (14 mil, 350 μm) silicon substrate at 30 GHz and at 10 GHz on thick high dielectric constant Duroid (ε_r= 10.5) [6]. In this paper, we show that micromachining can also improve a properly designed TSA which falls within the acceptable range of effective thickness'.

II. DESIGN

The TSA is designed to be $4\lambda_0$ long with a 12° flare angle, which results in an aperture of nearly $0.8\lambda_0$. The supporting material is 93mil thick (2.36mm) Duroid with an ε_r= 2.2. This results in a normalized effective thickness of 0.038, which is on the "high" side of values accepted for good operation. This design was expected to give acceptable performance with a gain on the order of 12 dB. The micromachined antenna has the same design except that the dielectric carrier has been machined with a periodic hole structure to disrupt the dominant substrate modes (Fig. 1).

Fig.1: Micromachined Tapered Slot Antenna

The holes are $0.1\lambda_0$ in diameter and spaced $0.17\lambda_0$ apart in a 2-dimensional fcc structure. This geometry was scaled from the 30 GHz silicon design where good results had already been observed. Specific design criteria for hole size and spacing has not yet been developed but it is expected to be completed for the conference (although it does appear that the symmetric fcc pattern will result in the best performance). The antennas were fed using a 0.085" (2.16 mm) coax line with the center conductor soldered across the slotline feed, which was shorted $\lambda_{guide}/4$ away for best transition performance.

III. MEASUREMENTS

The patterns measured for both the reference and micromachined antennas are shown in Figs. 2- 5 and summarized in Table 1.

	Reference	Micromachined
Directivity	15.4	17.0
-10 dB Beamwidth		
E-plane	40 °	38 °
H-plane	46 °	28 °
45° diagonal	50 °	20 °
X-Pol level (45 ° plane)	-10.4 dB	-7.3 dB
Main Beam η for an f/1 lens	83 %	86 %

Table 1: The measurement results at 10 GHz for the TSAs.

As shown, there is a significant improvement in the patterns in both the H-plane and 45°-diagonal plane. The increased sharpness will result in less spillover loss when feeding a lens. The overall improvement in the directivity would have been higher but there was an unexpected increase in cross-polarization levels in the micromachined antenna. Further investigation is needed, and it is expected that in the future the cross-polarization levels can be reduced,

resulting in an even higher directivity. The input impedance was measured using back-to-back antennas fed with the coax transition (Fig.6).The measurement technique used results in wideband information without the need of a large ground plane. However, the measured value is to Za/2, where Za is the input impedance of the TSA. The measured input impedance was found to be within 10% of the expected value, which is the impedance of the slotline feed (117 Ω in our case).

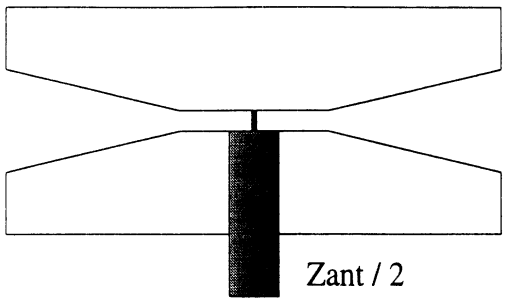

Fig.6: The impedance measurement technique used at X-band.

IV. Acknowledgements

This work is supported by the Army Research Office under the contract #DAAL04-94-G-0137. We would also like to thank Rogers Corp. for their support in supplying the dielectric material needed for the antennas.

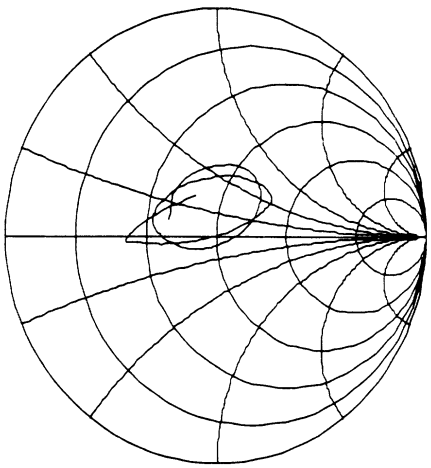

Fig.7: Measured input impedance of the reference TSA from 9-11 GHz.

REFERENCES

[1] Millitech Corp., South Deerfield, MA.
Contact: Dr. Richard Huguenin.

[2] TRW Corp., El Sigundo, CA.
Contact: Dr. Merit Schucri.

[3] K.S. Yngvesson *et al.*, "Endfire Tapered Slot Antennas on Dielectric Substrates," *IEEE Transactions Antenna & Propogation, vol.33 pp.1392-1400* December, 1985.

[4] E.R.Brown *et al.*, "Radiation Properties of a Planar Antenna on a Photonic-Crystal Substrate" *Journal of the Optical Society of America,* 1993.

[5] E.R.Brown *et al* , "High Zenith Directivity from a Dipole Antenna on a Photonic Crystal", submitted to *Applied Physics Letters.*

[6] T.J.Ellis and G.M.Rebeiz, "MM-Wave Tapered Slot Antennas on Micromachined Photonic Bandgap Dielectrics", to appear in the *IEEE-MTT* Symposium , June 1996.

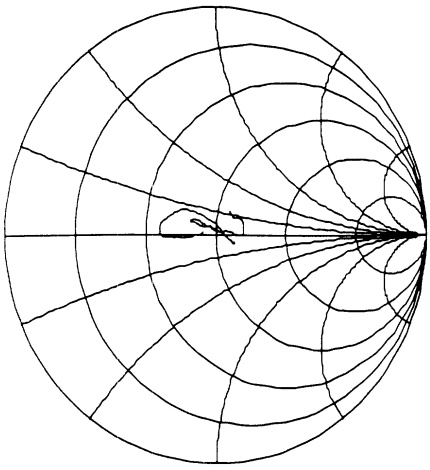

Fig.8: Measured input impedance of the micromachined TSA from 9-11 GHz.

INTEGRATION OF TAPERED SLOT ANTENNAS ON MMIC SUBSTRATES THROUGH DIELECTRIC MICROMACHINING

Thomas J. Ellis and Gabriel M. Rebeiz
Radiation Laboratory
University of Michigan
Ann Arbor, MI 48109

Abstract - A new type of dielectric substrate has been developed that can significantly improve the performance of tapered slot antennas and for the first time allow them to be integrated successfully onto the thick, high dielectric constant substrates used for commercial MMIC designs. The new substrate consists of a standard dielectric material that has been micromachined with a uniform, periodic series of holes. The effect of the micromachining is to artificially lower the dielectric constant of the substrate and to suppress the excitation and propagation of surface waves within the material. These two effects result in a 167% improvement in directivity and a 70% improvement in efficiency of a $4\lambda_0$ long TSA on a $0.14\lambda_d$ thick, $\varepsilon_r = 10.5$ dielectric substrate at 10 GHz. The micromachining can be achieved using standard via-hole processes resulting in low production costs. This technology can be scaled geometrically allowing for low frequency prototyping to be done inexpensively and later scaled up for high frequency applications such as imaging, radar, and power combining systems.

1. Introduction

The tapered slot antenna (TSA) was first introduced by Gibson *et al.* [1] in 1979. It consisted of a length of slotline printed on a dielectric substrate which flared outward along its length resulting in end-fire radiation (Figure 1). The TSA has many desirable properties which make it a popular choice for the design engineer. When properly designed it can have high directivity (10 - 20 dB) and efficiency (80% - 90%), with the E-plane and H-plane patterns being nearly symmetric in spite of the antenna being much thinner than it is wide. The fact that

it is a planar antenna makes it simple and inexpensive to fabricate and integrate monolithically with receivers and other systems, as well as form into 1 and 2 dimensional arrays. The limiting factor for using the TSA is the relative thickness of the dielectric substrate which they are fabricated on. An "effective" thickness has been previously defined to be

$$t_{eff} = t(\sqrt{\varepsilon_r} - 1)$$

which takes into account both the physical thickness and the relative dielectric constant of the substrate. Yngvesson *et al.*[2] have experimentally determined the range of normalized effective thickness for proper operation to be approximately

$$0.005 \leq \frac{t_{eff}}{\lambda_0} \leq 0.03$$

depending on the overall length of the antenna (the range given is for a TSA from about $4\lambda_0$ to $6\lambda_0$). If the antenna is made on a material that is thinner the main beam broadens and directivity is lost. Conversely, if the antenna is made on a thicker substrate surface waves develop which cause two different problems with the antennas performance. First, there is a reduction in efficiency associated with energy being coupling away from the desired radiated signal and into substrate modes. Second, when the surface waves that are excited reach the edges of the substrate they radiate. This undesired radiation can significantly interfere with the antenna, especially on boresight, and cause deep nulls in the resulting patterns.

The combination of the lower efficiency and poor patterns make the TSA an unacceptable option on the thick, high dielectric substrates that are used for monolithic circuits.

2. Micromachined Dielectrics

The dielectric substrate developed was bulk micromachined with a periodic series of via holes throughout the entire substrate (Figure 2). The process had two effects on the original dielectric material. The first is a lowering of the "effective" dielectric constant associated with the removal of material in the form of via holes. Several different geometrical placements were explored with their arrangements being shown in Figure 3. By defining a unit cell for each different arrangement simple volume calculations can be done to predict the dielectric constant of the micromachined structure. The "artificial" dielectric constant that results can be calculated using simple dielectric mixing models. A simple volumetric model was used and shown in Figure 4. Several experiments involving transmission lines and resonators were performed to verify the predicted values with the measured values being within 10 % of the predicted values for all cases. It is also interesting to note that a large range of dielectric constants can be synthesized through the control of hole diameter and spacing. This concept of

synthesizing an "artificial" dielectric constant has many applications both in and outside of planar antenna design.

The second effect that the micromachining has on the dielectric is to disrupt the formation and propagation of substrate modes (surface waves). When the TSA is fabricated on an electrically thick substrate, the slotline fields excite substrates modes that propagate within the dielectric. These unwanted fields are disruptive to the TSA operation as explained previously. To gain a better, although admittedly simplified understanding of the process of the surface wave disruption, a variation of the classic "grounded dielectric slab" problem was analyzed. If you approximate the micromachined substrate as a two dimensional grounded dielectric slab with a series of grooves etched into it (see Figure 5) the approximation is reasonably good if the holes are arranged so the surface wave effectively "sees" the same hole-gap structure in whatever direction it propagates. When the problem is solved the original boundary conditions remain with the addition of the continuity requirements in the propagation direction. The added boundary conditions are satisfied when

$$\underbrace{k_{z1}w}_{air\_gap} \geq \underbrace{k_0 w}_{free\_space} \sqrt{\varepsilon_r - 1}$$

with $k_{z1}w$ being the phase shift across the air gaps and $k_0 w$ being the phase shift across an equal physical distance in free space. For the surface wave to propagate

the holes must be small enough to get an "average" propagation constant throughout the material dominated by the remaining dielectric material. While this averaging is occurring the surface waves are "pulled" across the gaps by the fields in the remaining dielectric material. At some point the holes become too large for this to occur and, since a surface wave cannot propagate unguided through free space, propagation is stopped.

To support the above analysis, a simple experiment involving FEM analysis was constructed. Two dielectrically loaded waveguide were designed and analyzed from 1 to 12 GHz (see figure 6). The first was a reference X-band guide ($0.5\lambda_o$ long at 10 GHz) loaded with a uniform dielectric material with $\varepsilon_r = 10.5$. This was used to represent the surface waves in standard dielectric material. A waveguide structure was chosen because the TE_{10} mode is representative of the surface waves and numerically simple to solve. A second waveguide was constructed the same physical dimensions but with holes placed in the same orientation to the waveguide mode E-field as the surface wave would experience on the micromachined substrate. The resulting insertion loss for both simulations are displayed. The effect of the lower artificial dielectric constant can be seen in the shift of the lower frequency cutoff in the micromachined response. Also note that until a certain high frequency is reached both waveguides allow propagation with very low loss. The micromachined guide, however, shows the disruption the

holes have on propagation above a certain "cutoff" frequency in agreement with the previous analytical example.

3. Experimental Results

Several different TSAs were constructed, each having the same physical dimensions (see Figure 7) but with different hole orientations. The dielectric material used for all of the antennas was Duroid with a thickness of 50 mils (1270 μm) and a dielectric constant $\varepsilon_r = 10.5$. All of the antenna patterns were measured at the center design frequency of 10 GHz. The input impedance for the TSA is well behaved and approximately equal to the slotline feed impedance. Initial results agreed well with predicted impedance values so rigorous measurements were not taken.

As stated previously, the grounded dielectric slab problem is a simplified model for the actual micromachined dielectric. For the example to hold true the alignment of the holes must be made to closely resemble the periodic structure defined in the example (Figure 5). This suggests that the orientation of the holes controls the degree to which the surface waves are suppressed. This can be seen in the measured antenna patterns (Figure 8). For the same artificial dielectric constant ($\varepsilon_{eff} \approx 5$) the patterns change significantly as the hole geometry is varied. Since the greatest effect to the patterns from the surface waves occurs in the end-

fire direction, optimum performance is achieved by aligning the holes for maximum suppression in that direction (the "hexagonal" geometry). The directivity for each antenna was calculated using both co-pol and cross-pol measurements taken over a full 2π rotation. The results listed in Table 1 show that the improvement in performance is directly related to the hole placement (all of the antennas have approximately the same "artificial" dielectric constant).

Gain measurements were taken from 8.5 GHz to 12 GHz for three of the antennas. The results of the measurements are displayed in Figure 9. It is also important to note that the improvement is across a large bandwidth, indicating that the surface wave suppression is not a narrow-band resonant effect. The micromachined dielectric effectively utilizes the inherent wide-band performance of the TSA. With the gain and directivity measurements, the efficiency of the different antennas was computed (Table 2). As the material is changed from its reference (with no micromachining) to the "hexagonal" geometry the efficiency jumps dramatically approaching that of a TSA on thin, low ε_r Duroid, which was used as a reference goal for optimum performance.

Most of the initial fabrication and measurements for this research was done at 10 GHz. This simplified fabrication and testing and reduced any tolerance issues. The improvements due to micromachining are not, however, restricted to the lower frequencies. All of the different antenna designs were scaled

geometrically to 30 GHz and their patterns measured (Figure 10). The same improvements are seen as the hole geometry is varied, with a direct comparison between the two frequencies shown in Figure 11. The small difference in the patterns is attributed to a different measurement techniques, coaxial probing for the 10 GHz and diode detection at 30 GHz, and a small difference in scaling (the substrate was scaled by 70% while the frequency was scaled by 67%). It is clear from the comparison that this technique can be scaled consistently in frequency and there are no foreseeable problems with scaling to 60GHz or 94 GHz for high frequency Silicon or GaAs integrated circuits.

4. Conclusion

A new technique involving simple bulk micromachining has been presented that will allow, for the first time, the successful operation of tapered slot antennas on thick, high dielectric constant materials. Proper antenna operation is achieved through the combination of an artificially lowered dielectric constant and through surface wave suppression. The micromachining can be achieved using standard via-hole technology common to current MMIC fabrication processes which will allow for the improvements with little additional fabrication costs. The improvements gained through proper geometry design on the thick, high ε_r substrates allow the TSA to approach the performance of one designed on thin

low ε_r material. The technique has also been shown to be scaleable in frequency, allowing for simple and inexpensive low frequency prototyping to be done for very high frequency designs. The current work presented is currently being scaled to higher frequencies for radar, imaging and power combining applications.

5. Acknowledgments

This work was supported by The Army Research Office under the contract #DAAL04-94-G-0137. We would like to thank Rogers Corporation for their support in supplying the dielectric material needed for the antenna prototyping. We would also like to thank the other faculty members and graduate students of the Radiation Lab at the University of Michigan whose opinions and suggestions helped to make this work successful.

REFERENCES

[1] P.J.Gibson , "The Vilvaldi Aerial," *Proc. 9th European Microwave Conference,* 1979, pp.101-105

[2] K.S.Yngvesson *et al.* , "Endfire Tapered Slot Antennas on Dielectric Substrates," *IEEE Trans. Antennas & Prop.,* vol.33, pp1392-1400, Dec 1985

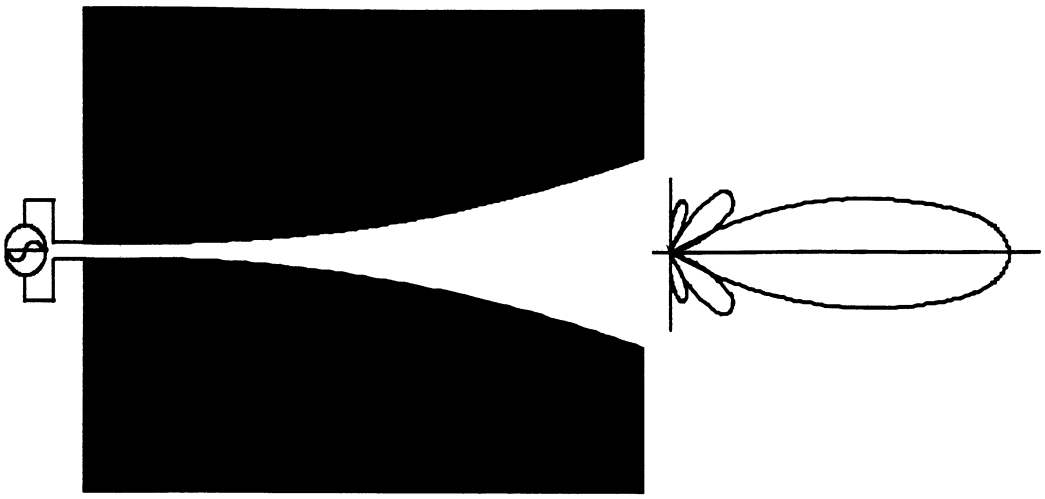

Figure 1. The "Vivaldi" tapered slot antenna.

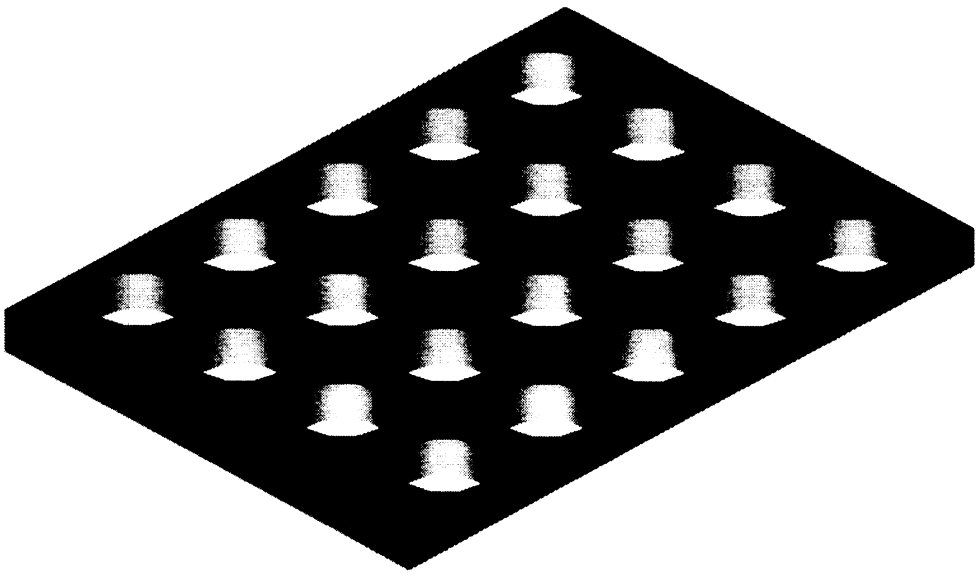

Figure 2. The micromachined dielectric substrate.

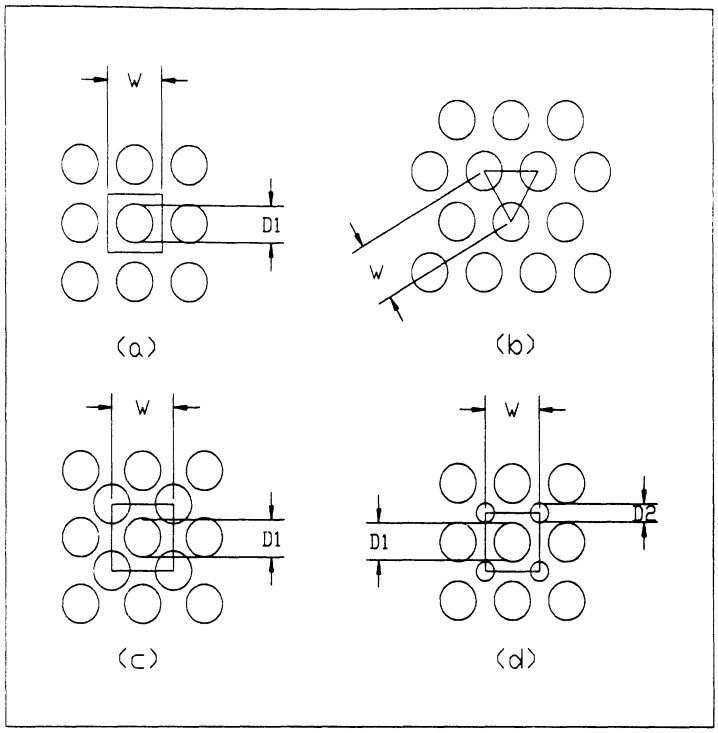

Figure 3. Unit cell definitions used to calculate the "effective" dielectric constant of the micromachined dielectric substrates. (a) Rectangular (b) Triangular (c) Hexagonal (d) Interlaced

Figure 4. Artificial dielectric constant calculated using a simple mixing model for the "Hexagonal" geometry.

Submitted to IEEE Trans. on Antennas and Propagation, June 1998

MM-Wave Tapered Slot Antennas on Synthesized Low Permittivity Substrates

Jeremy B. Muldavin, *Student Member, IEEE,*
and Gabriel M. Rebeiz, *Fellow, IEEE.*

Abstract— This paper presents 30 GHz linear tapered slot antennas (LTSA) and 94 GHz constant width slot antennas (CWSA) on synthesized low dielectric constant substrates. The performance of tapered slot antennas is sensitive to the effective thickness of the substrate. We have reduced the effective thickness by selectively machining holes in the dielectric substrate. The machined substrate antenna radiation patterns were significantly improved independent of the machined hole size or lattice as long as the quasi-static effective thickness remained the same, even if the hole/lattice geometry is comparable to a wavelength. The method was applied at 94 GHz on a constant width slot antenna with excellent far field pattern improvement, making it suitable for f/1.6 imaging array applications.

Index Terms---micromachining, artificial substrates, tapered slot antennas.

I. Introduction

Tapered Slot Antennas (TSA) have been developed by Gibson et. al [1] and Yngveson et. al [2,3] for phased array and focal plane imaging systems. The performance of a TSA is sensitive to the thickness and dielectric constant of the antenna substrate. An *effective thickness*, which represents the electrical thickness of the substrate, has been defined as $t_{eff} = t\left(\sqrt{\varepsilon_r} - 1\right)$. One accepted range of the effective thickness (determined experimentally) for good operation of a TSA is given as $0.005\lambda_0 \le t_{eff} \le 0.03\lambda_0$ [2]. For substrate thickness above the upper bound of effective thickness, unwanted substrate modes develop which degrade the performance of the tapered slot antenna, while antennas on thinner substrates suffer from decreased directivity.

The upper bound on the effective thickness, $t_{eff} \le 0.03\lambda_0$, necessitates mechanically thin substrates for mm-wave applications, even if low dielectric constant materials are used. For example, a maximum thickness of $200\mu m$ (8 mils) is allowed for a 94 GHz TSA integrated on an $\varepsilon_r = 2.2$ dielectric substrate. This results in a mechanically fragile substrate.

One way of improving the mechanical stability is to increase the thickness of the substrate and then selectively remove parts or nearly all of the underlying dielectric material. If nearly all of the substrate is removed, the TSA can be suspended on a thin dielectric membrane with an effective dielectric constant of $\varepsilon_r = 1.05$ [4]. This is easily implemented at sub mm-wave frequencies (300 GHz - 3 THz), but is not as practical at mm-wave frequencies (30-300 GHz) since the membrane dimensions are large and the mechanical stability of the suspended membrane is compromised. Other researchers (Vowinkel et al [5]) have selectively removed large portions of the dielectric inside the slot area of the TSA with good results.

In this work, an array of closely drilled holes is used to remove a portion of the underlying substrate, thereby resulting in a lower quasi-static (effective) dielectric constant substrate. This technique has been applied successfully using microstrip antennas [6]. The volume of the dielectric removed can be precisely controlled (between 0-100%) and determines the effective dielectric constant of the substrate. In this application, around 40-50% of the substrate is removed to maintain good mechanical properties.

II. 30 GHz Design & Measurements

A. LTSA Design

A non-optimal linear tapered slot antenna design, shown in figure 1, was chosen for the 30 GHz experiments. The LTSA was designed to be $4\lambda_0$ long with a 12° taper angle, which results in nearly one λ_0 aperture. The slotline feed was $200 - 300\mu m$ wide. The substrate is 1.27 mm (50 mils)

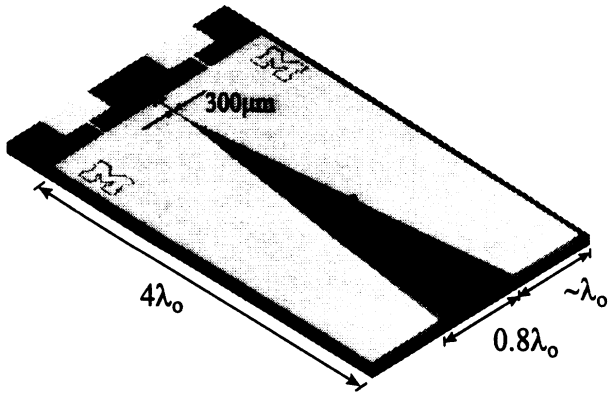

Figure 1 The linear tapered slot antenna on a 1.27 mm thick RT/duroid ($\varepsilon_r = 2.2$) substrate. The pads on the end of the antenna are for low frequency signal pickup.

EECS Department
The University of Michigan
Ann, Arbor, MI 48109-2122

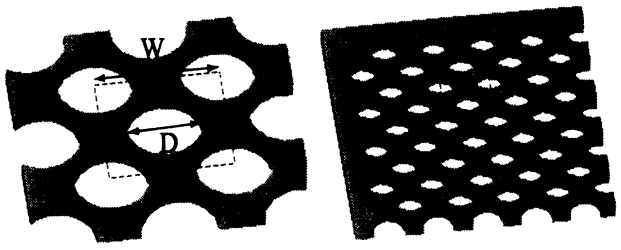

Figure 2. Hole patterns machined into the substrates of the 30 GHz tapered slot antennas. The larger pattern has a hole diameter, D, of 3.18 mm (125 mils), and a spacing, W, of 5.08 mm (200 mils). The smaller pattern has hole diameters of 1.27 mm (50 mils), and spacing of 2.03 mm (80 mils). The dashed box represents the unit cell.

thick RT/duroid, with a relative dielectric constant of $\varepsilon_r = 2.2$. Three different substrates were investigated: *solid substrate*, *big hole substrate*, and *small hole substrate*. The big hole and small hole patterns, shown in figure 2, were machined in a 45-degree rotated rectangular lattice with an automated milling machine. The big hole substrate was chosen to be a large fraction of a wavelength with $D = \lambda_o/3$ (3.18 mm) and $W = \lambda_o/2$ (5.08 mm). The small hole pattern was chosen with $D = \lambda_o/8$ (1.27 mm) and $W = \lambda_o/5$ (2.03 mm). Previous measurements at 10 and 30 GHz have shown that the lattice choice (rectangular, hexagonal, etc.) has no effect on the far field patterns for low dielectric constant substrates [7].

The machined substrates were chosen to have the same effective relative dielectric constant. The effective dielectric constant is a quasi-static value, given by the volumetric average dielectric constant of the machined substrate, and is: $\varepsilon_{eff} = \frac{\pi}{2}\left(\frac{D}{W}\right)^2 + \varepsilon_r\left[1 - \frac{\pi}{2}\left(\frac{D}{W}\right)^2\right]$, where D and W are defined in figure 2.

For RT/duroid, with $\varepsilon_r = 2.2$, the effective dielectric constant, ε_{eff}, is equal to 1.46 for the two machined substrates shown in figure 2. For a 30 GHz TSA integrated on 1.27 mm (50 mils) thick substrate, this reduction in the effective dielectric constant changes the value of t_{eff}/λ_0 from 0.061 for the solid substrate to 0.026 for the machined substrates, placing the effective thickness just within the performance limits of Yngveson et al [2].

B. 30 GHz Measurements

The normalized radiation patterns of the antennas were measured in an anechoic chamber. The thin leads and the pads on the slot end of the antenna (Fig. 1) were designed to allow pickup of low frequency signals from a zero-bias Schottky diode (Metelics MSS20141-B10D, $C_j = 0.8pF$) placed over the slot line of the antenna, one quarter of a guided wavelength from a capacitive RF short. The RF source was AM modulated at 5 kHz and radiated by a standard gain horn. The detected low frequency signal (5 kHz) at the diode terminals was delivered to a lock-in amplifier. The amplified signal was then read by a computer, which controled the antenna mount positioner.

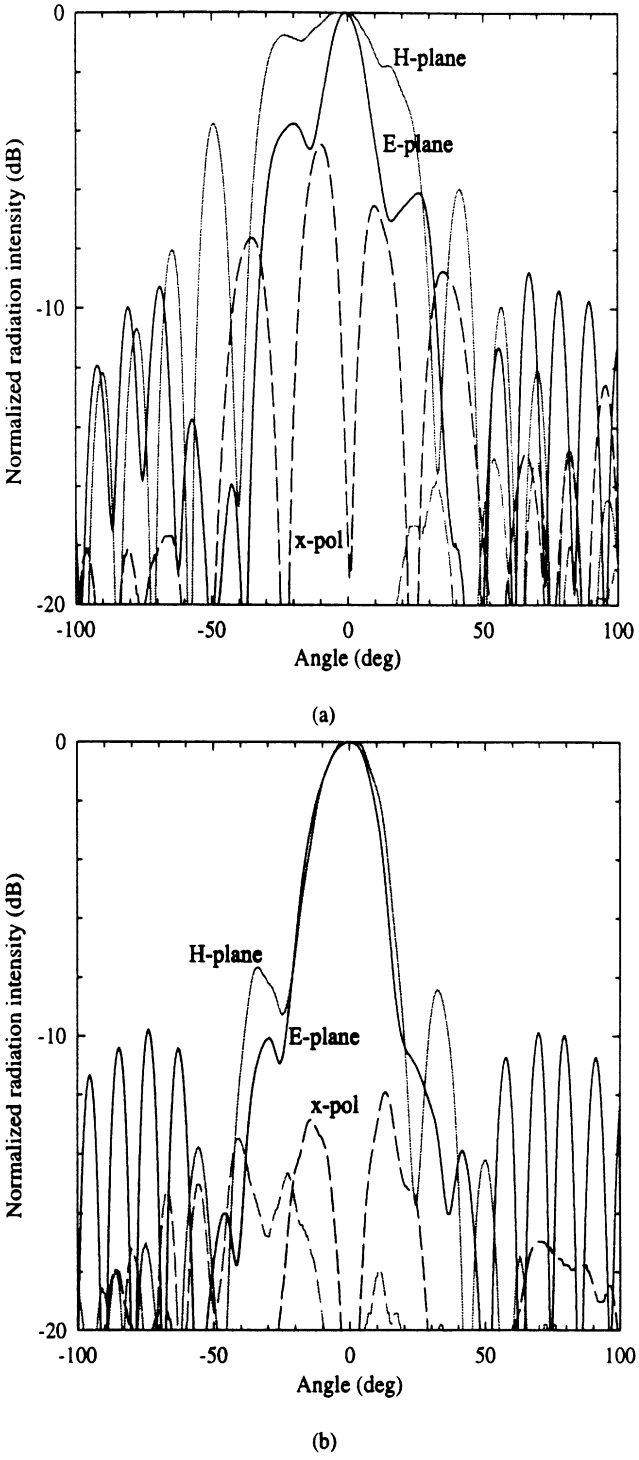

Figure 3. Measured 30 GHz far field antenna patterns for the solid substrate (a) and the big hole LTSA (b).

The 30 GHz far field radiation patterns of the solid substrate and the big hole substrate antennas are shown in figure 3. There was significant improvement in the far field patterns of both the E- and H-plane with the machined substrates. Note the lower cross-polarization levels in the E- and H-plane patterns for the machined big hole antenna. No directivity values are quoted since the 45°-plane co- and cross-polarization patterns were not measured. The big hole and the small hole tapered slot antennas gave very similar patterns to within ±1° and ±1dB (Fig. 4). This indicates that the improvement in performance is independent of hole

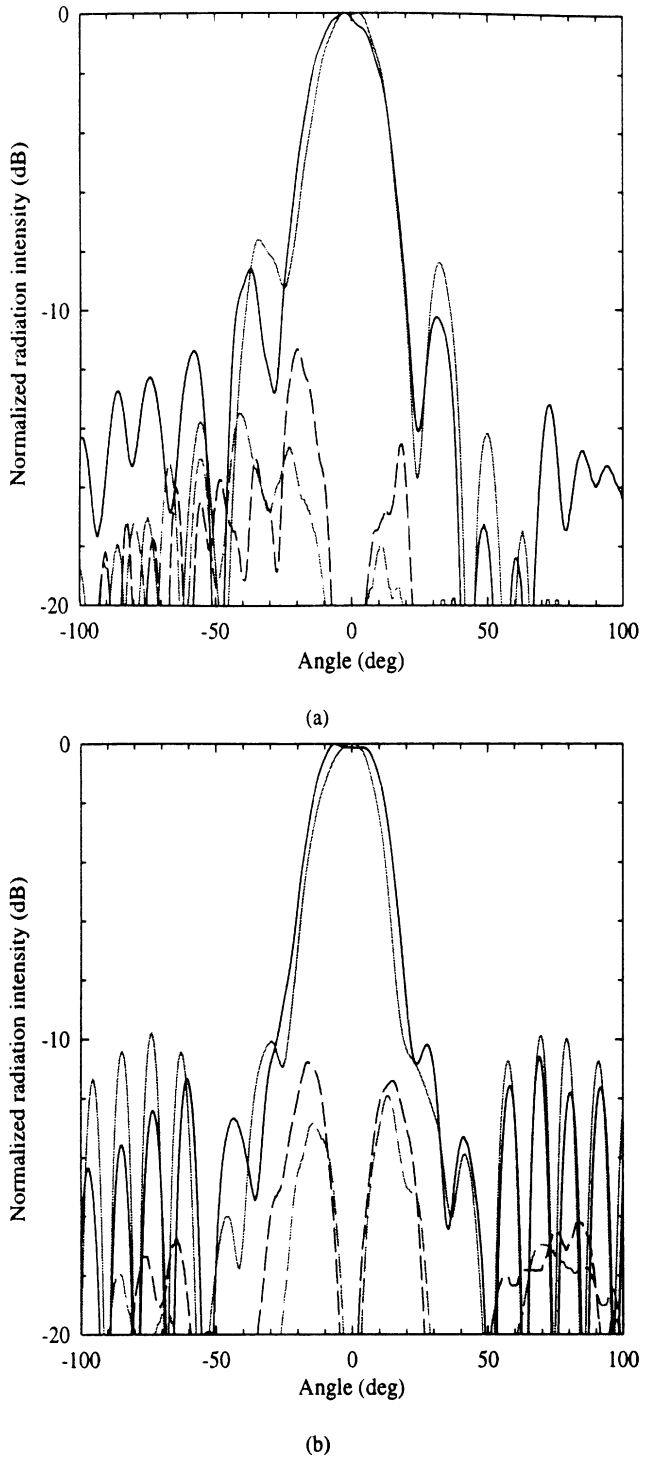

Figure 4. Measured 30 GHz H-plane (a) and E-plane (b) far field pattern measurements for the big hole (gray) and the small hole LTSA (black).

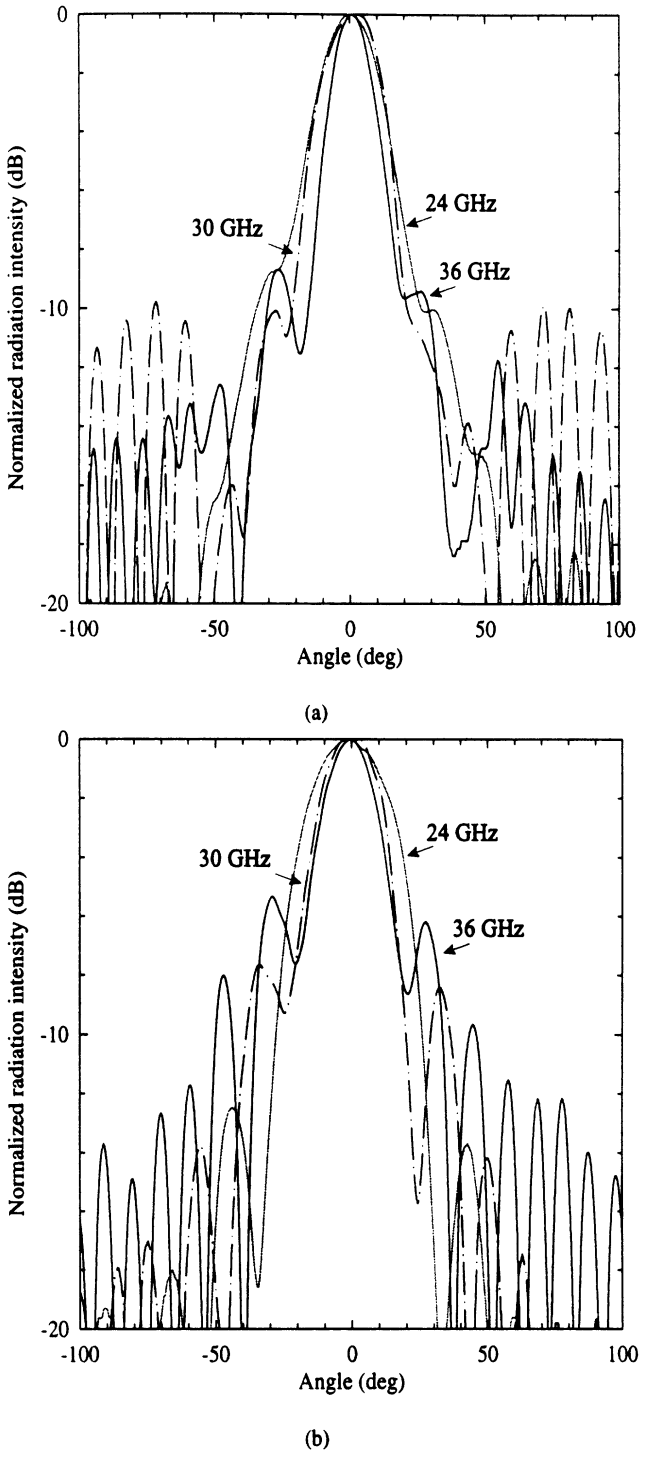

Figure 5. Measured 24 (gray), 30 (dash-dot) and 36 (solid) GHz E-plane (a) and H-plane (b) far field co-polarization antenna patterns for the big hole LTSA.

Table 1. Comparison of the 3-dB and 10-dB beamwidths for three different 30 GHz TSA substrates.

Antenna	3-dB		10-dB	
	E-plane	H-plane	E-plane	H-plane
Solid substrate	17	54	66	67
Big/small hole	25	26	42	43

geometry even if the holes/periods are a large fraction of a wavelength. This further suggests that the effect is purely a quasi-static reduction of the substrate dielectric constant, and not a mode suppression/photonic bandgap mechanism typically seen in high dielectric constant substrates [7].

The 3-dB and 10-dB beamwidths for all three antennas are summarized in Table 1. Notice the fine structure (or ripple) in the measured patterns at angles above ±40°. This is believed to be an interference pattern from the measurement setup and the edge of the TSA substrate. Recently, Sugawara et al. have shown that TSA patterns are very sensitive to currents induced on the edge of the finite-width substrate. These edge currents are in opposite phase to the slot-antenna currents and result in interference-like patterns at large measurement angles [9]. The big hole

antenna results in symmetrical patterns at 30 GHz, and for a 10-dB taper in an imaging lens system, the antenna will fit an f/1.25 lens.

A comparison of the measured 24, 30, and 36 GHz far field radiation patterns for the big hole antenna is shown in figure 5. The backside radiation patterns ($|\theta| \geq 90^{\circ}$) were below −15 dB. The peak cross-polarization levels were below −12.5, -10.5, and -8.5 dB at 24, 30, and 36 GHz, respectively. The corresponding patterns of the small hole LTSA are virtually identical and are not shown. As the frequency increases, the beamwidth decreases, the side lobe levels increase, and the patterns degrade as the effective thickness increases (as expected). Note that even at 36 GHz with $D = \lambda_o/2.5$ and $W = \lambda_o/1.6$, the big hole TSA gave virtually identical patterns to the small hole TSA with $D = \lambda_o/6.3$ and $W = \lambda_o/4$.

III. 94 GHz Design & Measurements

A. 94 GHz Design

A constant width tapered slot antenna design, provided by Dr. Ellen Moore at Millimetrix Corporation, was used for the 94 GHz experiments (Fig. 6). In order to obtain and effective thickness of $t_{eff} \leq 0.03\lambda_o$ at 94 GHz, the solid substrate thickness must be less than $200\mu m$, resulting in a mechanically unstable substrate. Increasing the thickness to $380\mu m$ (15 mils) improves the mechanical stability to a practical level. We compared $380\mu m$ thick solid substrate antennas to antennas machined with a hole pattern, shown in figure 2, having a diameter of $380\mu m$ ($\lambda_o/9$) and a spacing of $610\mu m$ ($\lambda_o/5$). In retrospect, these dimensions were chosen to be unnecessarily small and can easily be enlarged by a factor or 2-3. The machining removes approximately 40% of the substrate and again results in an effective dielectric constant of 1.46. The effective thickness of the antenna is reduced from 0.058 to 0.025, again just within the acceptable limits.

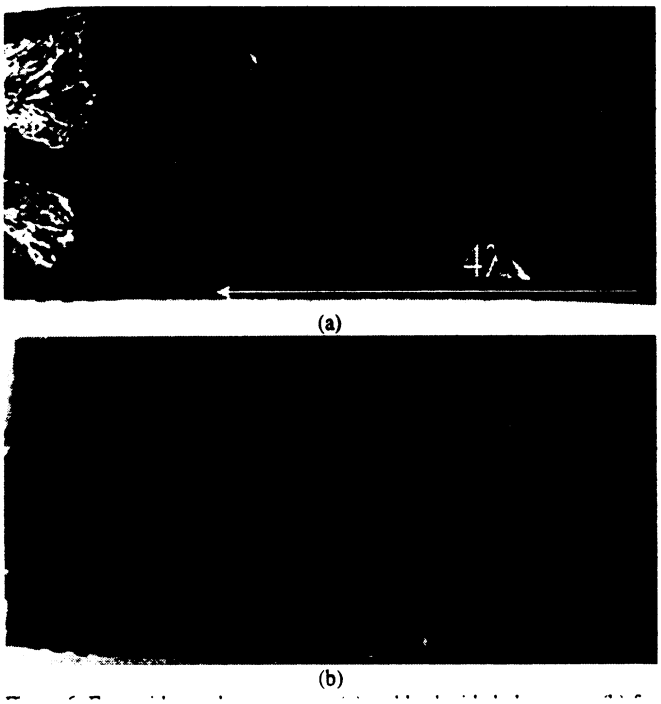

(a)

(b)

B. 94 GHz Measurements

The 94 GHz measurements were performed on a bench top with absorber placed around the perimeter of the bench.

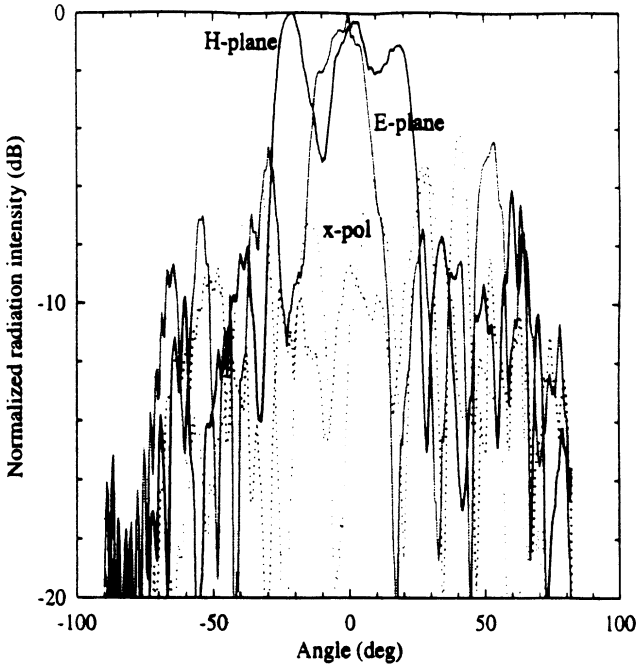

(a)

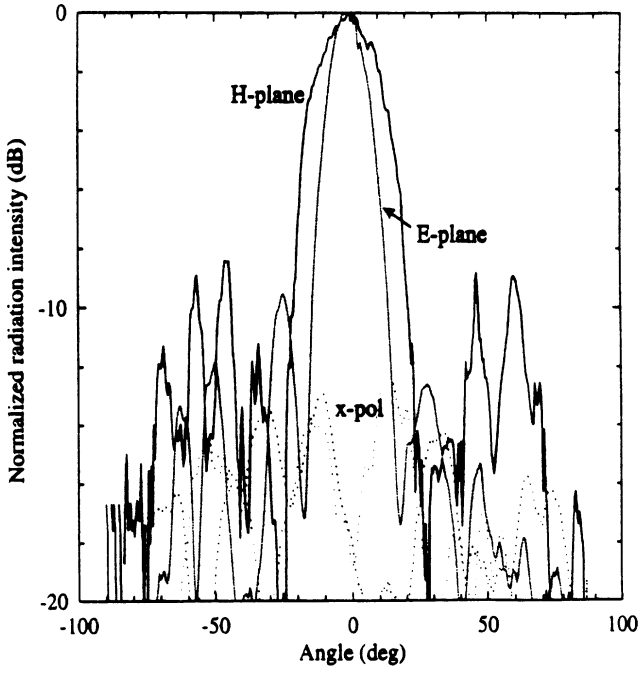

(b)

Figure 7. Measured 94 GHz solid substrate (a) and machined substrate antenna (b) far field co-polarization and cross-polarization antenna patterns.

The measurements were performed with an experimental setup similar to the 30 GHz setup, except with an AM modulated 94 GHz Gunn-diode source. An Alpha diode (DMK2784-000, $C_j = 0.04pF$), placed across the slot, was used to detect the modulated signal. A signal to noise ratio of greater than 20 dB was achieved.

The 94 GHz far field antenna patterns for the solid substrate and the machined CWSA are shown in figure 7. The CWSA showed excellent pattern improvement for the machined case, with low cross polarization levels (-13 dB). The sharp -10 dB sidelobes are believed to be due to the edge currents on the finite width ($0.5\lambda_o$) conductor half plane. The machined CWSA results in an average -10 dB beamwidth of 35° and fits an f/1.6 lens imaging system.

IV. Conclusions

We have shown that selective machining of a thick dielectric substrate results in a simple method for reducing the effective thickness of tapered slot antennas. If low dielectric constant substrates are used, the improved far field radiation patterns are not sensitive to hole geometry or lattice choice (as long as the quasi-static effective thickness remains the same) and can be easily scaled with frequency from 10-94 GHz. A 94 GHz constant width tapered slot antenna on a $380\mu m$ thick machined substrate ($\varepsilon_r = 2.2$) was successfully fabricated, showing mechanical stability and practical radiation performance, for imaging array applications.

V. Acknowledgments

This work has been supported by the US-Army Research Office under an AASERT (DAAL04-94-G-0137) and under a subcontract from Millimetrix Corporation.

VI. References

[1] P. J. Gibson , "The Vivaldi Aerial," *Proc. 9th European Microwave Conference*, 1979, pp.101-105.

[2] K. S. Yngvesson et al., "Endfire Tapered Slot Antennas on Dielectric Substrates," *IEEE Transactions Antenna & Propogation*, vol. 33 pp. 1392-1400 December, 1985.

[3] K.S.Yngvesson et al., "The Tapered Slot Antenna - A New Integrated Element for MM Wave Applications", *IEEE Trans. Microwave Theory & Tech.*, vol. 37, pp.365-374, Feb. 1989.

[4] P. R. Acharya et al., "Tapered Slotline Antennas at 802 GHz", *IEEE Trans. Microwave Theory & Tech.*, vol. 41, pp.1715-1719, Oct. 1993.

[5] U. K. Kotthaus and B. Vowinkel, "Investigation of Planar Antennas for Submillimeter Receivers", ", *IEEE Trans. Microwave Theory & Tech.*, vol. 37, pp.375-380, Feb. 1989.

[6] G. P. Gauthier, A. Courtay, and G. M. Rebeiz, "Microstrip Antennas on Synthesized Low Dielectric-Constant Substrates", *IEEE Trans. On Antennas and Propagation*, vol. 45, pp.1310-14-380, Aug. 1997.

[7] T. J. Ellis and G. M. Rebeiz, "MM-Wave Tapered Slot Antennas on Micromachined Photonic Bandgap Dielectrics" *IEEE-MTT Symposium*, San Francisco, pp. 1157-1160, June 1996.

[8] T. J. Ellis and G. M. Rebeiz, "Improvements in Tapered Slot Antennas on Thick Dielectric Substrates Using Micromaching Techniques" *IEEE Int. Symposium on Antennas and Propagation*, Baltimore, pp. 992-995, July 1996.

[9] S. Sugawara et al.., "Characteristics of a MM-Wave Tapered Slot Antenna with Corrugated Edges", " *IEEE-MTT Symposium*, Baltimore, June 1998.

IEEE International Symposium on Antennas and Propagation, Montreal, July 1997, pp. 1110-1113

Tapered Slot Antennas on Thick Dielectric Substrates Using Micromachining Techniques

Jeremy B. Muldavin, Thomas J. Ellis and Gabriel M. Rebeiz

Electrical Engineering and Computer Science Department
University of Michigan, Ann Arbor, Michigan 48109
muldavin@engin.umich.edu, tellis@engin.umich.edu, rebeiz@engin.umich.edu

Abstract- Tapered Slot Antennas operating at 35 GHz were fabricated on thick (50 mils, 1.27 mm) low dielectric constant (ε_r = 2.2) substrate using micromachining techniques. Several periodic hole structures were machined into the substrate and the resulting antenna pattern measurements were compared. The micromachining of the substrate improves the antenna patterns. The mechanism of improvement is believed to be the reduction in the effective dielectric constant of the substrate. This work is being extended to 94 GHz for application in an imaging array.

I. Introduction

The performance of the Tapered Slot Antenna (TSA) is sensitive to the thickness of the supporting substrate. Development of a mechanically stable substrate would be advantageous for many practical applications of the TSA. An "effective thickness" can be defined as

$$t_{eff} = t\left(\sqrt{\varepsilon_r} - 1\right)$$

and represents the electrical thickness of the substrate. One accepted range of the effective thickness [1] for good operation of a TSA is given as

$$0.005 \le \frac{t_{eff}}{\lambda_o} \le 0.03 .$$

For substrate thickness above the upper bound on performance, unwanted substrate modes may develop which degraded the performance of the antenna. The upper bound on this range requires mechanically thin substrate for high frequency applications , e.g. t_u = 198 μm (7.8 mils) for a 94 GHz TSA integrated on ε_r = 2.2 Duroid. Increasing the mechanical thickness of the substrate while keeping the electrical thickness within the accepted limits of operation may allow for practical application of these antennas to imaging arrays, etc.

In this paper, it is shown that micro-machining a periodic hole pattern into a mechanically-thick low-dielectric substrate of a TSA will allow acceptable operation of the antenna. We believe that the major cause of the improvement of the operation with micro-machining is the reduction of the relative dielectric constant due to the reduced relative volume of the dielectric to air.

II. Design/Experimental Setup

The TSA is designed to be $4\lambda_o$ long with a 12° taper angle, which results in an aperture of nearly $0.8\lambda_o$. Figure 1 shows the conductor pattern geometry. The supporting material is 50 mil thick Duroid with an ε_r = 2.2. Three different substrate geometries were investigated: "No Hole Pattern", "Big Hole Pattern", and "Small Hole Pattern". The Big Hole and Small Hole Pattern geometries are shown in Figure 2.

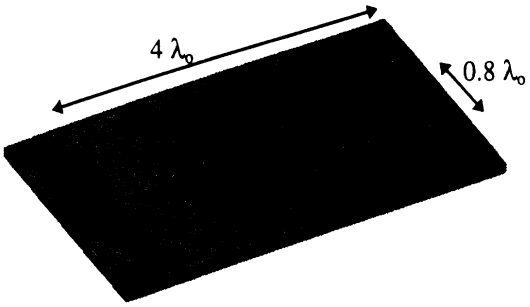

Fig. 1 *The conductor pattern of the micro-machined tapered slot antenna on a 50 mil thick Duroid substrate. The pads on the end of the antenna are for low frequency signal pickup.*

The micro-machined geometries were chosen to have the same effective relative dielectric constant. The effective dielectric constant is a quasi-static value, given by the volumetric average dielectric constant of the micro-machined substrate, and is given by the following formula:

$$\varepsilon_{reff} = \frac{\pi}{2}\left(\frac{D}{W}\right)^2 + \varepsilon_r\left(1 - \frac{\pi}{2}\left(\frac{D}{W}\right)^2\right),$$

where D and W are defined in Figure 2.

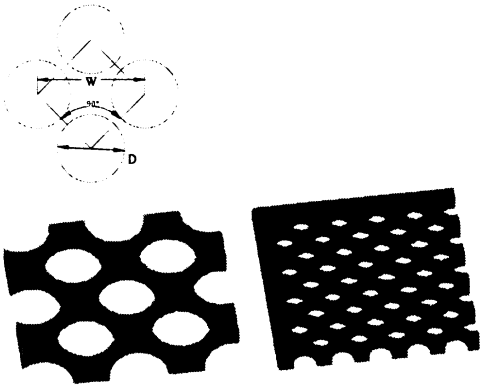

Fig. 2 *Hole patterns micro-machined into the subsrates of the tapered slot antennas. The larger hole pattern has a hole diameter, D, of 3.175 mm (125 mils), and a spacing, W, of 5.08 mm (200 mils). The smaller hole pattern has hole diameters of 1.27 mm (50 mils), and spacing of 2.032 mm (80 mils).*

For Duroid, ε_r=2.2, the effective dielectric constant, ε_{reff}, is equal to 1.46 for the two micro-machined geometries that were chosen. For a 35 GHz TSA integrated on 50 mil thick ε_r=2.2 Duroid, this reduction in the effective dielectric constant changes the value of t_{eff}/λ_0 from 0.0716 for the No Hole Pattern to 0.0309 for the micro-machined hole patterns, placing them just within the performance limits

The measurement setup is shown in Figure 3. The thin leads and the pads on the slot end of the antenna (Fig. 1) are designed to allow pickup of low frequency signals from a zero-bias Schottky diode (Metelics MSS20, 141-B10D, C_t=0.8 pF, R_V=2 kΩ) placed over the slot line of the antenna, one quarter of a guided wavelength ($\lambda_g/4$) from a RF short (Fig. 3). The low frequency signal (5 kHz) is delivered to a lock-in amplifier. The amplified signal is then read by a computer, which also controls the antenna mount positioner.

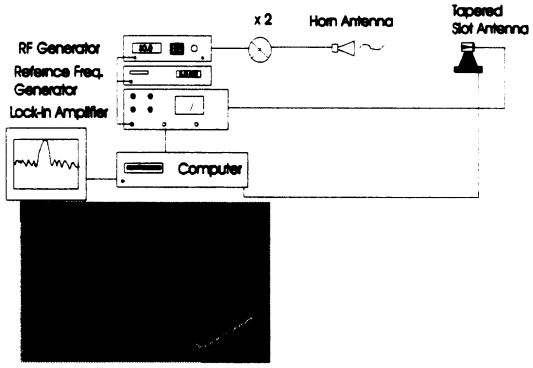

Fig. 3 *Measurement Setup. The signal from the tested antenna is detected using a zero-bias Schottky diode placed over the slot line of the antenna as shown. An RF short is placed over the end of the slot line to prevent leakage of radiation from the rear of the antenna.*

III. Measurements

The patterns measured at 30 GHz for all three antennas are shown in Figure 4. The 3-dB and 10-dB beamwidths for all three antennas are summarized in Table 1. As shown, there is significant improvement with micro-machining in the patterns in both the E- and H-planes. The Big Hole and the Small Hole Pattern

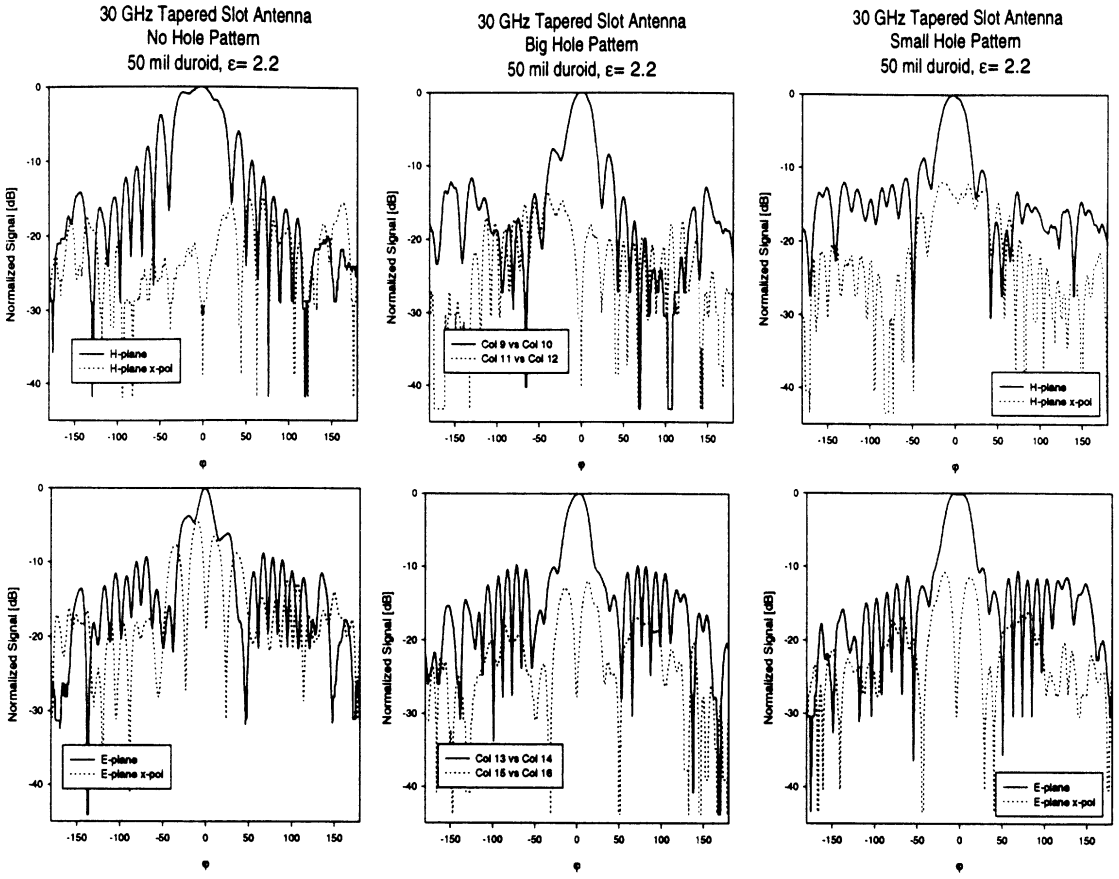

Fig. 5 *Antenna pattern measurements for the No Hole antenna , Big Hole antenna, and the Small Hole antenna at 30 GHz. Note that the normalized signal, not an absolute gain is plotted versus angle. The Big Hole antenna and the Small Hole antenna both give similar improvements from the No Hole antenna.*

Table 1. *Angular beamwidths for selected antennas.*

		3-dB Beamwidth (°)		10-dB Beamwidth (°)	
Antenna	Frequency (GHz)	E-plane	H-plane	E-plane	H-plane
No Hole	24	24	31	70	80
	30	17	54	66	67
	36	16	36	53	69
Big Hole	24	26	34	61	54
	30	25	26	42	58
	36	17	22	44	69
Small Hole	24	25	37	55	56
	30	30	28	50	47
	36	19	24	39	40

TSAs gave very similar results. Notice the fine structure (or ripple) in the measured patterns at angles above |±40°|, which is believed to be an interference pattern from the measurement setup. Also note the low cross-pol. levels in the E- and H-plane patterns for the micro-machined Big Hole antenna. The Big Hole antenna results in symmetrical patterns at 30 GHz, and for a 10-dB taper in an imaging lens system, the antenna will fit an f/0.75-f/0.8 lens.

Due to the ripple in the measurements, we have not measured the 45°-plane patterns and therefor cannot calculate the directivity for the measured patterns explicitly. However, we can apply an approximate formula which results in an upper estimate of the directivity value.

$$D \cong \frac{32{,}400}{\phi_E \phi_H},$$

where ϕ_E , ϕ_H ≡ 3-dB beamwidths in the E- and H-plane patterns, respectively. At 30 GHz, D is equal to 50 (17 dB) and 35 (15.4 dB) for the Big Hole and No Hole antennas, respectively. This is only an estimate and assumes a Gaussian-type beam pattern with low cross-polarization levels. It is expected that the correct directivity of the antennas will be 2-3 dB lower than the values given above.

The micro-machining results in good antenna patterns up to 36 GHz for this design, and since the scaling laws were already verified with photonic-bandgap antennas, we expect that the 94 GHz versions will produce similar results.

IV. Future Work

We believe that the interference structures result from both a pickup in the low frequency lines and large reflection at the slot line/diode interface. As is known, a zero-bias diode detector has an impedance of ~100 kΩ, resulting in a very high reflection coefficient. In order to solve this, the diode will be biased at 0.12 mA so as to result in a junction resistance of 200 Ω. Also, a cpw to slot line transition will be used to extract the low frequency component in a low radiation cpw line. This will eliminate any pickup from the low frequency side of the circuit.

V. Acknowledgments

This work is supported by the Army Research Office under the contract #DAAL04-94-G-0137. We would also like to thank Rogers Corporation for their support in supplying the dielectric material needed for the antennas.

REFERENCES

[1] K. S. Yngvesson et al., "Endfire Tapered Slot Antennas on Dielectric Substrates," *IEEE Transactions Antenna & Propogation*, vol. 33 pp. 1392-1400 December, 1985.

[2] T. J. Ellis and G. M. Rebeiz, "Improvements in Tapered Slot Antennas on Thick Dielectric Substrates Using Micromaching Techniques" *IEEE Int. Symposium on Antennas and Propagation*, Baltimore, July 1996.

[3] T. J. Ellis and G. M. Rebeiz, "MM-Wave Tapered Slot Antennas on Micromachined Photonic Bandgap Deilectrics" *IEEE-MTT Symposium*, San Francisco, June 1996.

FINAL REPORT

94 GHz PHOTONIC BANDGAP TAPERED SLOT ANTENNAS

Period Covered: 14 Aug. 1996-18 May 1997

Perpared by:

J. Muldavin and G. Rebeiz
Radiation Laboratory
University of Michigan
Ann Arbor, MI 48109
rebeiz@engin.umich.edu

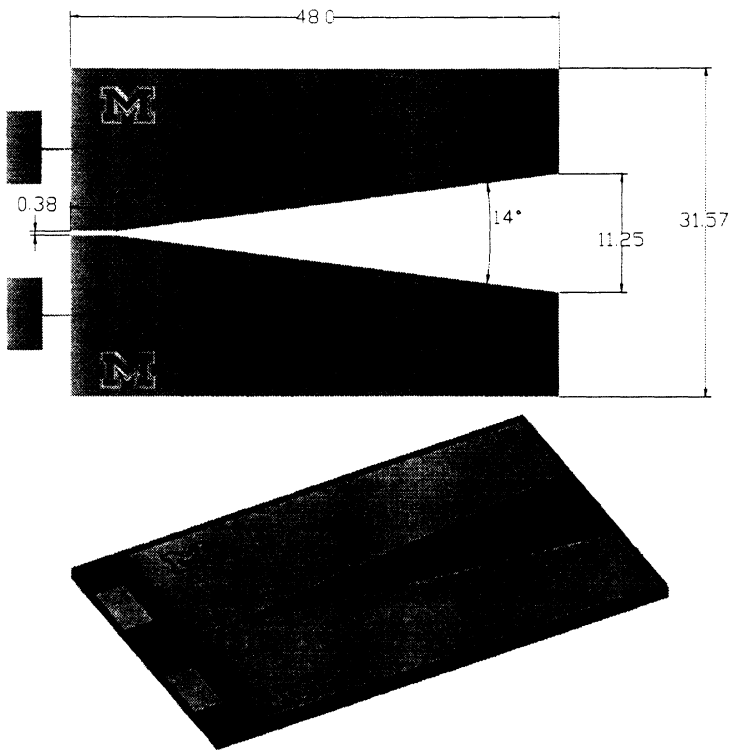

Fig. 1 *Conductor pattern for micro-machined tapered slot antennas. The patterns were designed on AutoCad and machined using QuickCircuit and a CAM milling machine. The antennas were designed to operate around 30 GHz. (Dimensions in mm).*

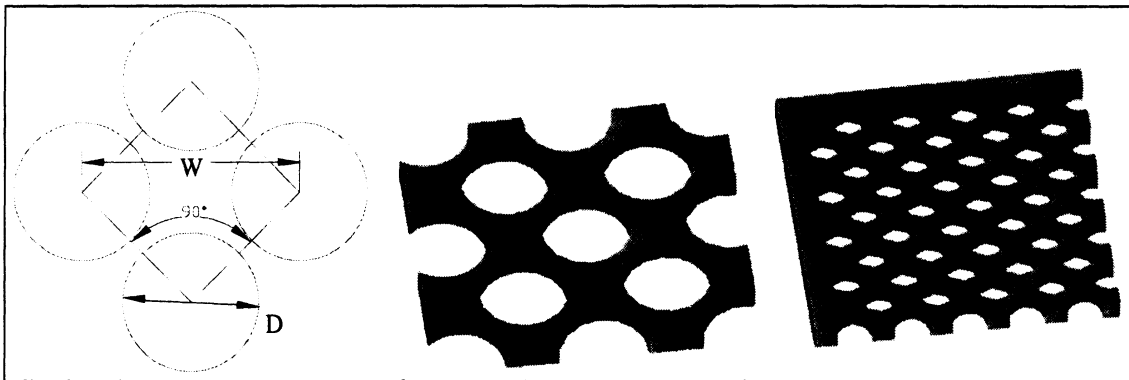

Fig. 2 *Hole patterns micro-machined into the subsrates of the tapered slot antennas. The larger hole pattern has a hole diameter, D, of 3.175 mm (125 mils), and a spacing, W, of 5.08 mm (200 mils). The smaller hole pattern has hole diameters of 1.27 mm (50 mils), and spacing of 2.032 mm (80 mils).*

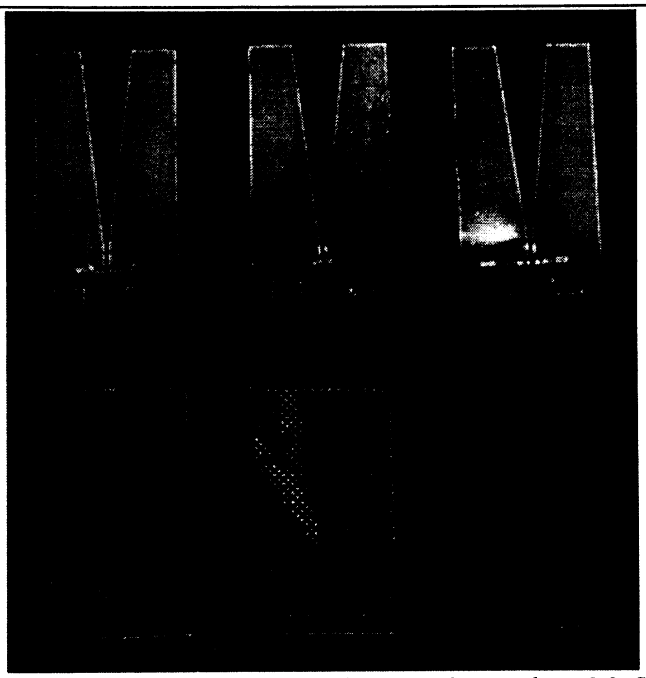

Fig. 3 *Micro-machined tapered slot antennas fabricated on 50 mil Duroid, ε_r=2.2. Shown from left to right are the Big Hole pattern, Small Hole patter and No Hole pattern antennas, top and bottom views. If you look carefully, you can see a trace of the conductor pattern through the machined substrates.*

Table 2. *Angular beamwidths for selected antennas.*

		3-dB Beamwidth (°)		10-dB Beamwidth (°)	
Antenna	Frequency (GHz)	E-plane	H-plane	E-plane	H-plane
No Hole	24	24	31	70	80
	30	17	54	66	67
	36	16	36	53	69
Big Hole	24	26	34	61	54
	30	25	26	42	58
	36	17	22	44	69
Small Hole	24	25	37	55	56
	30	30	28	50	47
	36	19	24	39	40

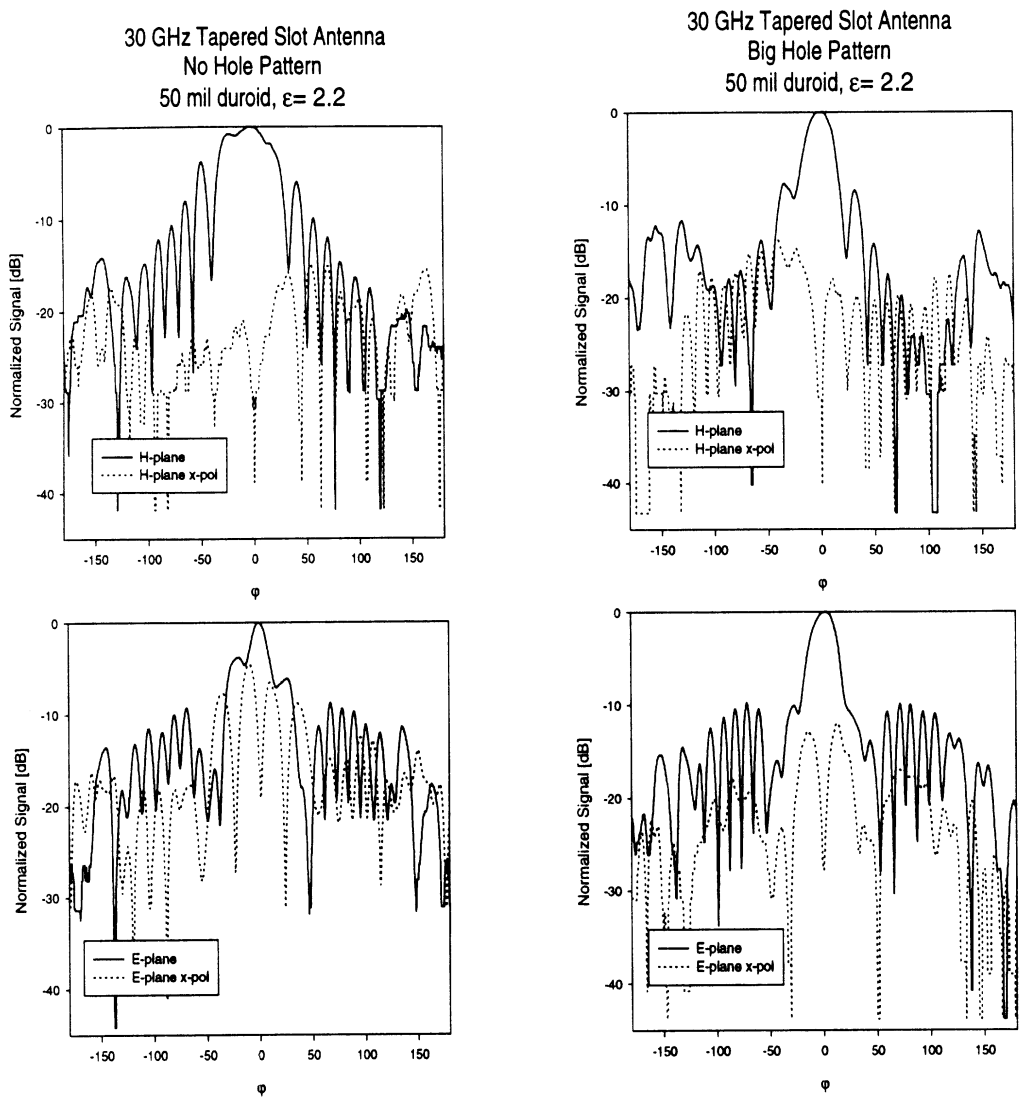

Fig. 5 *Antenna pattern measurements for the No Hole antenna and the Big Hole antenna* at 30 GHz. Note that the normalized signal, not an absolute gain is plotted versus angle.

Milimetrix Constant Width Antenna
10 GHz Scaled Model
60 mil, 2.5 Duroid
machined 125/200

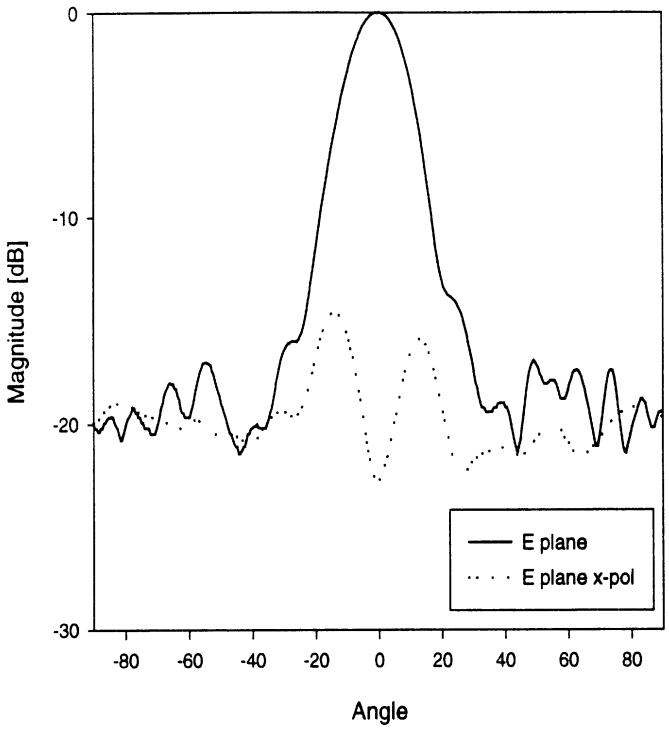

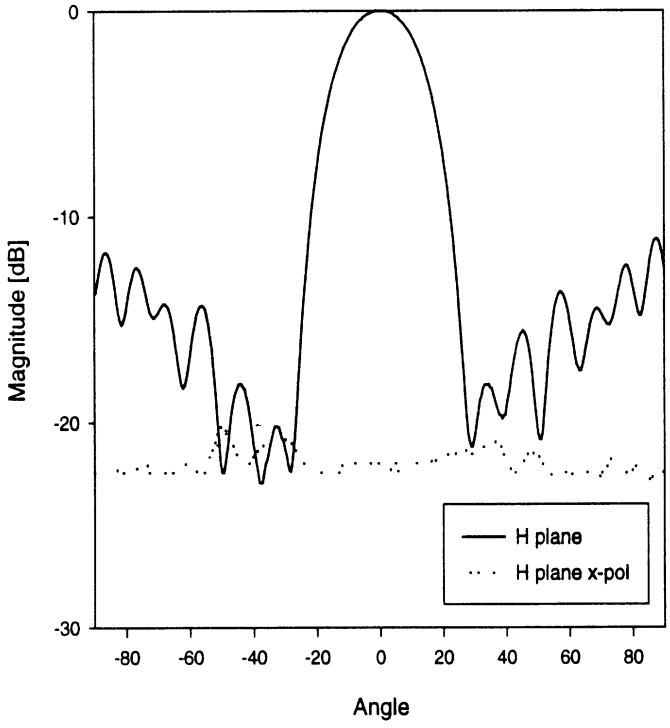

Milimetrix Constant Width Antenna
94 GHz
17 mil, 2.2 Duroid
machined 15/24

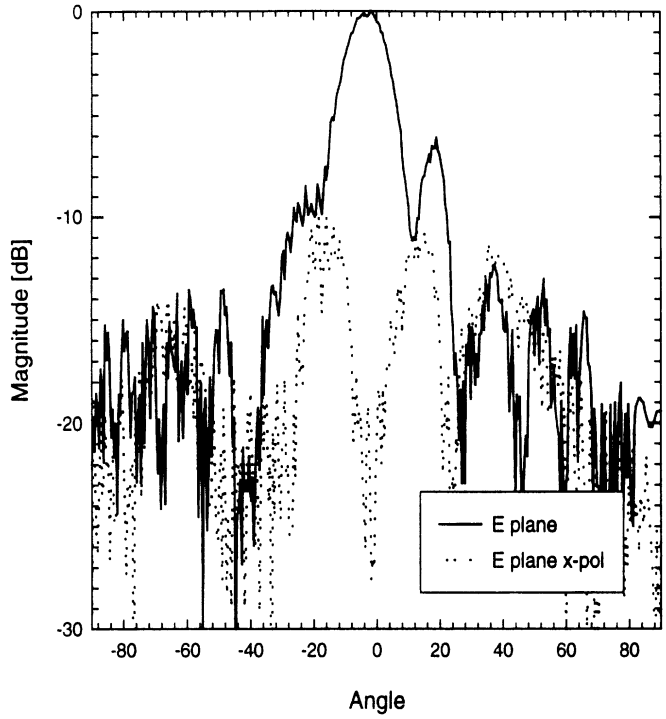

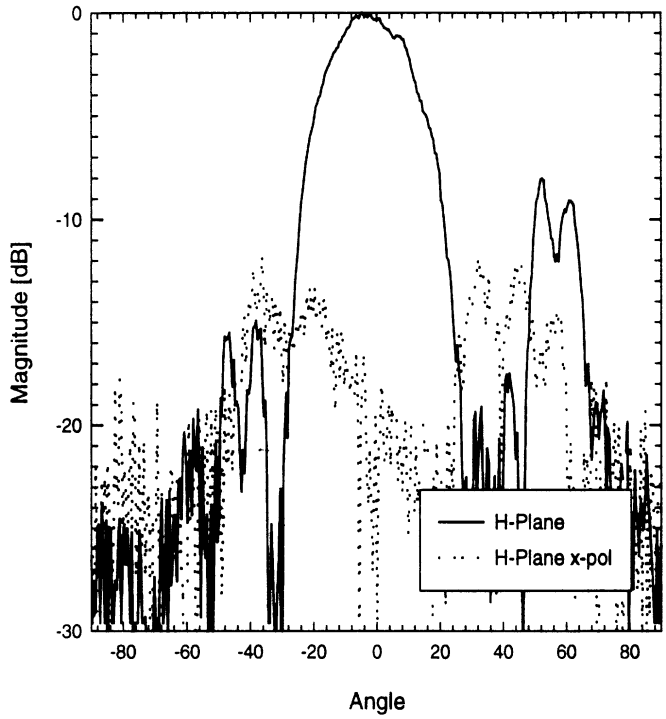

Milimetrix Constant Width Antenna
46.5 GHz
17 mil, 2.2 Duroid
Machined 15/24